

# **ENGR 490 FINAL DESIGN REPORT**

Solar Panel Cleaning Drone

**By:**

Raad Haider (40209418) – AERO ENG – raad.haider02@gmail.com

Aysenur Kocak (40206455) – AERO ENG – aysenurk25@hotmail.com

Oumaima Hida (40213345) – AERO ENG – oumaima.hida.02@gmail.com

Nadim Zreik (40208567) – AERO ENG – nadimz101@gmail.com

Aidan Mulrooney Gélinas (40208123) – AERO ENG – aidanpatmg@gmail.com

Qian Yi Wang (40211303) – COMP ENG – qianywang25@gmail.com

Philip Carlsson-Coulombe (40208572) – COMP ENG –  
philipcarlssoncoulombe@gmail.com

**Submitted to:**

Krzysztof Skonieczny



Concordia University

Montreal, QC, Canada  
April 14<sup>th</sup>, 2025

## **Abstract**

This project aims to develop a semi-autonomous system for cleaning rooftop solar panels that prioritizes environmental sustainability, safety, and efficiency. The project consists of a flying drone and an autonomous cleaning rover, designed to address issues associated with traditional manual cleaning methods, such as high labor costs, safety risks, and limited access to hard-to-reach areas.

The mandate is as follows:

1. Define and establish regulatory and market requirements aligned with industry standards.
2. Integrate advanced technologies to enhance operational performance and precision.
3. Design and develop an autonomous navigation and cleaning system.
4. Design a reliable payload transport and deployment system.
5. Validate the design through testing to ensure safety, durability, and compliance with regulations.

The project offers a safer, more affordable, and ecologically friendly alternative to current solar panel cleaning techniques by delivering a stable drone and an autonomous rover equipped with effective cleaning technologies and traction systems. This solution optimizes energy efficiency and supports the adoption of renewable energy technologies.

## Table of Contents

Abstract .....	2
List of Figures .....	5
List of Tables .....	7
1. Introduction.....	8
2. Literature Review.....	9
2.1. Movement System .....	9
2.2. Drone Release and Capture Mechanism .....	9
2.3. Cleaning System .....	9
2.4. Edge Detection System.....	9
2.5. Positioning System.....	9
3. Main Project Requirements.....	10
4. Final Design .....	12
4.1. Drone Design .....	12
4.1.1. Propeller and Motor Selection .....	12
4.1.2. Release and Capture Mechanism .....	13
4.1.3. Drone Flight Controller.....	14
4.1.4. Drone Structural Design .....	15
4.1.5. Drone System Components.....	16
4.1.6. Drone Landing Gear Design .....	16
4.2. Rover Design .....	17
4.2.1. Rover Fuselage.....	17
4.2.2. Track System .....	18
4.2.3. Cleaning System .....	21
4.2.4. Autonomous Control System.....	22
4.2.5. Rover System Components .....	23
4.3. Drone Manufacturing.....	24
4.4. Release and Capture Mechanism .....	24
4.4.1. Drone System Manufacturing .....	25
4.5. Rover Manufacturing .....	25
4.5.1. Rover Fuselage.....	25
4.5.2. Displacement System.....	26
4.5.3. Cleaning System .....	27
4.5.4. Rover System Integration .....	28
4.6. Design Validation and Testing.....	29
4.6.1. Propeller Testing.....	29
4.6.2. Flight Tests .....	30

4.6.3.    Release Mechanism Testing (Aidan).....	31
4.6.4.    Rover Testing .....	32
4.7.    Design Deviation .....	37
4.8.    Final Product .....	39
5.    Cost Breakdown.....	42
6.    Entrepreneurship and Logistics.....	46
6.1.    Potential Customers and Investors.....	46
6.2.    Funding Sources.....	46
6.3.    IP and Patent Issues .....	47
6.4.    Competitors.....	47
6.5.    Product Life-Cycle Analysis.....	47
7.    ELSEE Aspects .....	48
8.    Safety and Risk Assessment .....	52
9.    Lessons Learned.....	55
10.    Conclusion .....	56
References.....	57
Appendix A.....	58
Appendix A contd.....	59
Appendix B .....	60
Appendix C .....	62
Appendix D .....	63
Appendix E .....	64
Appendix F.....	65
Appendix G.....	67
Appendix H.....	68
Appendix I .....	69
Appendix J .....	70
Appendix K.....	71
Appendix L .....	76

## List of Figures

Figure 1: SPCD Mission Plan Overview.	8
Figure 2: Release Mechanism, Counter-bored and Counter-sunk Fastener Holes.	13
Figure 3: Release Mechanism, Magnet Fastening and Wire Channel.	13
Figure 4: Release Mechanism Final Design CAD.	13
Figure 5: Controller with Fully Assembled Electronics Box.	15
Figure 6. CAD Assembly of the Drone.	15
Figure 7: Drone Stack and Electronics CAD.	16
Figure 8: Drone Landing Platform CAD.	16
Figure 9: Rover Assembly CAD.	17
Figure 10: Detailed drawing of the rover.	17
Figure 11: Rover Fuselage and Cover CAD.	18
Figure 12: Rover Wheel Encoder and Motor Brackets.	18
Figure 13: CAD of the Rover Displacement System.	19
Figure 14: Rover Driven Shaft CAD.	19
Figure 15: Final Brush System CAD.	21
Figure 16: First Frozen Back Cloth CAD.	21
Figure 17: User Flow for Autonomous Rover Behavior.	22
Figure 18. Rover System Components CAD.	23
Figure 19: Drone and Electronics Fully Assembled.	24
Figure 20: Assembled Release Mechanism.	25
Figure 21: Printed Rover Fuselage and Modifiable Brackets.	26
Figure 22: Physical Assembly of the Rover Displacement System.	26
<i>Figure 23: Manufacturing Process of the Rover Timing Belts.</i>	27
Figure 24: Soft Bristle Brush, Before Manufacturing.	27
Figure 25: Final Physical Assembly of the Brush System.	27
Figure 26: Second Design for the Back Cloth Rod.	28
Figure 27: Final Physical Assembly for the Back Cloth Rod.	28
<i>Figure 28: Rover Wiring for Testing.</i>	29
Figure 29: Propeller Testing Stand Assembly.	29
Figure 30: Broken Propeller After Initial Flight Test.	30
Figure 31: Drone Assembly with Legs.	31
Figure 32: Release Mechanism Weighted Test.	32
Figure 33: Rover Simulation - Motor Step Response and PID Tracking.	33
Figure 34: Rover Simulation - IMU Noise.	34
Figure 35: Rover Simulation – Encoders.	35
Figure 36: Rover Simulation - Track PIDs with Encoders.	35
Figure 37: Rover Simulation - Orientation PID.	36
Figure 38: Rover Simulation - Positional PID.	36
Figure 39: Rover Simulation - Limit Switches.	36
Figure 40: Rover Simulation Complete Mission Path.	37
Figure 41. Evolution of the Tracks, [A] TPU Tracks [B] Mold and Silicone Tracks [C] Comparison [D] Molding Process.	38
Figure 42. Design Iterations of The Rover Track Mount.	38
Figure 43: Final Drone Model.	39
Figure 44: Final Rover Model on Solar Panels.	40
Figure 45: Rover attached to the release mechanism (with the temporary landing gear legs).	40
Figure 46: Rover On Top of Solar Panels.	40
Figure 47: SPCD Team Presenting the Final Product at the Capstone Design Presentation on April 1st.	41

Figure 48: Cost of Change as Design Progresses. ....	42
Figure 49: Drone Cost Breakdown Pie Chart. ....	43
Figure 50: Rover Cost Breakdown Pie Chart. ....	44
Figure 51: The SPCD Team at Bell Textron. ....	46
Figure 52: 3D Printing Tolerance Testing Board. ....	50
Figure 53: Risk Assessment List and Mitigation Plans. ....	52
Figure 54: Risk Severity Grids. ....	53
Figure 55. Scope and Design Evolution of the SPCD Project.....	55
Figure 56. Team Breakdown Structure.....	58
Figure 57. Work Breakdown Structure.....	59
Figure 58. Detailed Drawing of the Drone. ....	64
Figure 59: Landing Gear Assembly Drawing.....	65
Figure 60: Landing Gear Drawing - Rod Center .....	65
Figure 61: Landing Gear Drawing - Rod Slot .....	66
Figure 62: Landing Gear Drawing - Rod Strut .....	66
<i>Figure 63: Detailed drawing of the rover fuselage .....</i>	67
Figure 64: Detailed Drawing of the Rover Displacement System.....	68
Figure 65: Brush System Drawing.....	69
Figure 66: Back Cloth Drawing.....	70
Figure 67: Complete Rover Systems KiCad. ....	71
Figure 68: Power System Rover KiCad. ....	71
Figure 69: Track System KiCad. ....	72
Figure 70: Rotary Encoder System KiCad.....	72
Figure 71: Cleaning System KiCad. ....	73
Figure 72: Edge Detection KiCad. ....	74
Figure 73: Radio Module KiCad.....	75
Figure 74: Complete Drone System KiCad. ....	76
Figure 75: Radio Module KiCad.....	76
Figure 76: Flight KiCad. ....	77
Figure 77: Release Mechanism KiCad. ....	77
Figure 78: Drone Power KiCad. ....	78

## List of Tables

Table 1: Motor and Propeller Selection .....	12
Table 2: Release Mechanism Component Selection.....	14
Table 3: Release Mechanism Final Design Specifications.....	14
Table 4: Drone Frame Specifications. ....	15
Table 5: Drone and Payload Mass Budget.....	16
<i>Table 6: General Calculated Parameters for the Track System Sizing .</i>	18
Table 7: Gear Bending Stress Calculation.....	20
Table 8: Comparison of Yield Strength and Margin of Safety for Aluminum Alloy and Steel. .....	20
Table 9: Magnet Strength Testing Results.....	31
Table 10: Rover Simulation Mission Time.....	37
Table 11. Mass Breakdown Of The SPCD.....	41
Table 12: Drone Cost Breakdown via Excel.....	43
Table 13: Rover Cost Breakdown via Excel.....	44
Table 14 Expenses Excel .....	45
Table 15: ELSEE Stakeholders Overview.....	48
Table 16: R&D Trends with Competitors.....	49
Table 17: ELSEE Compliance Decisions. ....	50
Table 18: FHA for the Drone.....	54
Table 19: FHA for the Rover. ....	54
Table 20: Breakdown of Main Requirements for All Subsystems. ....	60
Table 21: High Level System Requirements. ....	62
Table 22: Subsystem Requirements.....	63

## 1. Introduction

### Market Analysis

Rooftop solar panels are an efficient and sustainable way to generate electricity, reducing carbon emissions and energy costs. With a global market size of USD 101.55 billion in 2022, it is projected to grow to USD 434.63 billion by 2032 at a 15.7% compound annual growth rate [1], maintaining these panels is critical to maximizing their potential. However, soiling, caused by dirt, dust, and debris, can reduce energy output by up to 25% [2]. Traditional cleaning methods are labor-intensive, costly, and require safety measures, especially for high or hard-to-reach rooftops.

### Project Objectives

This project aims to develop a semi-autonomous tool capable of cleaning solar panels placed on high rooftops and hard-to-access areas. The solution will be composed of two main entities: a flying drone and a panel cleaning robot. An operator will pilot the drone to reach the panels and allow the robot to autonomously clean each panel. The drone must maintain stability while flying and hovering, with and without the robot's added weight. The secondary robot is required to ensure the safety of the panels, reduce the operator's workload, ensure full coverage of the panels, and reduce the power consumption of the drone. The mission plan of the proposed product is represented in Figure 1. A detailed organization of the project is provided in Appendix A.

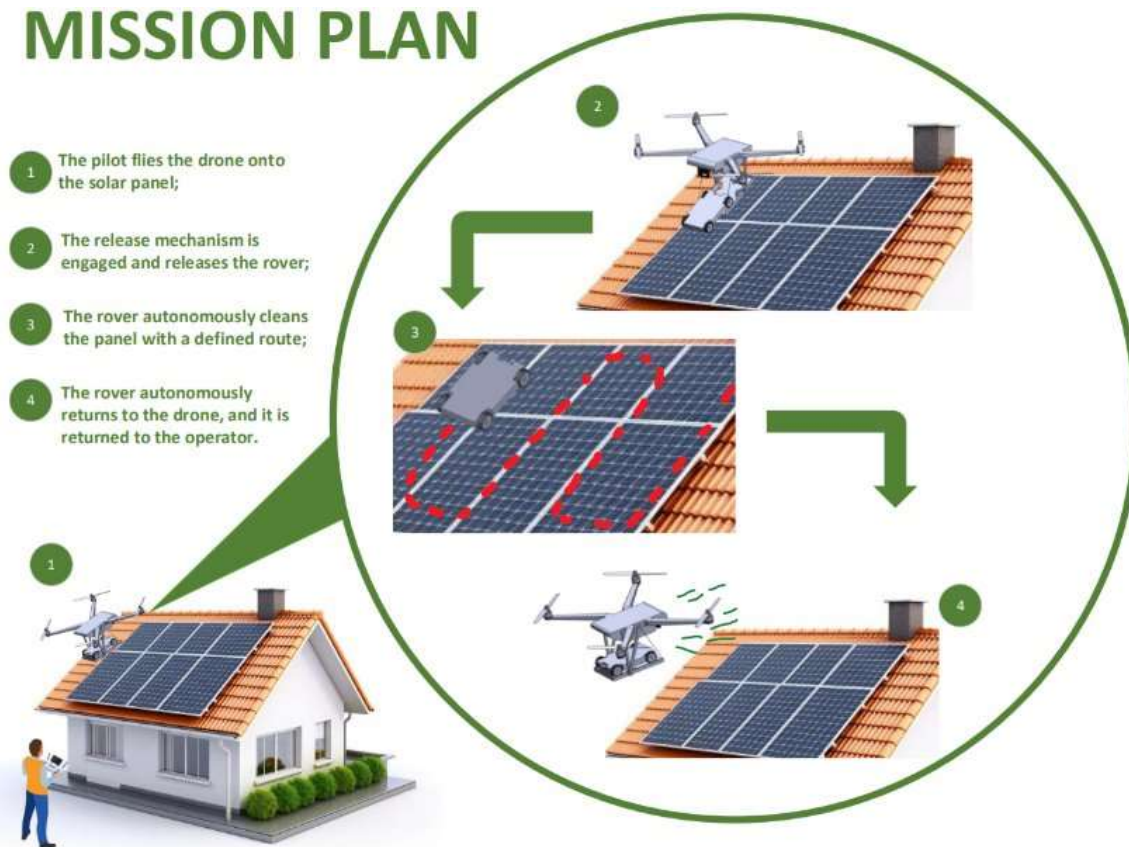


Figure 1: SPCD Mission Plan Overview.

## 2. Literature Review

In this section, a summary of the components that were ultimately selected for the final design is presented. Building upon the design considerations and evaluations conducted earlier in the project, the final choices were made based on performance, reliability, and complexity. The selected components include the movement system, drone release and capture mechanism, cleaning system, edge detection system, and positioning system. These choices reflect the most suitable options identified through decision matrices and detailed analysis, ensuring an effective overall system.

### 2.1. Movement System

For the cleaning system, differential steering was selected. This choice stood out for its strong terrain compatibility and excellent maneuverability, especially on inclined solar panel surfaces. In addition to its performance benefits, this option offered a lower overall cost compared to more complex alternatives. To further improve grip and durability, silicone-molded tracks were chosen for the final design due to their flexibility, grip as well as durability.

### 2.2. Drone Release and Capture Mechanism

To securely deploy and retrieve the cleaning robot, the team opted for a magnetic attachment system using 12V DC 25N electromagnets. This approach provided a simple yet effective solution that minimized mechanical complexity while still ensuring a strong and stable connection between the drone and rover during flight and landing operations.

### 2.3. Cleaning System

To clean the solar panels effectively without risking surface damage, a combination of microfiber cloth and bristle brushes was selected. This provided a high level of cleaning efficiency while remaining lightweight and easy to integrate into the rover. While water-based cleaning methods were considered, they were ultimately dismissed due to the added weight and limited improvement in performance.

### 2.4. Edge Detection System

The rover employed an edge detection system to prevent it from falling off rooftops. This system consisted of four pairs of limit switches (eight in total), with each pair containing an outer and inner switch. The outer switch detected when the rover approached the edge, while the inner switch confirmed that the edge had been reached. This setup enabled the rover to navigate around the perimeter of the solar panel array without relying on GPS or cameras.

### 2.5. Positioning System

Position tracking was achieved through the use of an IMU for orientation, wheel encoders for velocity and distance, and the limit switches for edge detection. These components worked together to estimate the rover's location while compensating for drift. This allowed the system to perform accurate, GPS-free navigation across rooftop solar panel installations.

### 3. Main Project Requirements

Design requirements are essential specifications that drive the scope of the project. Each subsystem of the technology has its own set of requirements defining its capabilities, functionalities and characteristics. A table combining all the requirements can be found in Appendix B.

**Law and Regulations Requirements:** One of the categories refers to the laws and regulations that the drone must follow to ensure safe operation, prevent potential hazards and avoid interference with restricted airspace. These regulations also address privacy concerns and compliance with local aviation authority. An example would be that the drone shall not fly within 3 nautical miles of an airport or 1 nautical mile of a heliport.

**Weight Requirements:** The weight requirements ensure that the subsystems remain within the payload capacity of the drone and the cleaning rover to optimize flight stability, energy efficiency and safe transport. An example of such requirement would be that the maximum takeoff weight of the drone shall not exceed 6kg.

**Cleaning System Requirements:** The cleaning system requirements focus on ensuring effective debris removal without damaging the panels, while cleaning in a reasonable amount of time. An example of cleaning requirement would be that the cleaning rover shall be capable of effectively removing dust, bird droppings, and leaves from solar panel surfaces to ensure optimal performance without damaging the surface of the panels.

**Track System Requirements:** The track system requirements ensure smooth and reliable movement of the rover across solar panels, prioritizing features such as lightweight, anti-slip designs for traction on solar panel surfaces, and a pressure distribution mechanism to prevent damage to the panels while maintaining stability and efficiency during operation. One of the requirements is the traction system shall carry the rover's weight without slipping at maximum angles of 25°.

**Release Mechanism Requirements:** The release mechanism requirements focus on ensuring a safe and reliable detachment of the rover from the drone to the solar panel. This includes a plate equipped with magnets and motorized pivoting system that securely holds the rover in place during transport and smoothly releases it without sudden movements or damage to the panels, while also being able to withstand mechanical stresses during the flight and deployment. An example of requirement would be that the release mechanism shall be equipped with 4 Uxcell 12V 25N lifting magnets able to lift the cleaning rover to and from the solar panels.

**Drone Requirements:** The drone requirements aim to safely transport and deploy the rover onto the solar panels. Some key considerations include sufficient payload capacity, stable flight performances and precise control for accurate positioning and release of the rover. Additionally, the drone should be capable of withstanding environmental conditions such as moderate winds and varying temperatures. An important drone requirement to take into consideration during the design is that the propellers must be capable of generating sufficient thrust (2700 g each) to lift the drone with its payload, ensuring stable flight performance across various operating conditions.

System requirements are broken down into high-level categories and specific subsystem requirements. The high-level requirements focus on broad system functions, reliability, and power management, emphasizing overarching goals and capabilities. Subsystem requirements are more specific and detail how each functional component should perform within the system.

A summary is provided below. For a more detailed visualization of requirements, refer to Appendix C for a list of high-level system requirements and Appendix D for the subsystem requirements list.

**Functionality:** The functional requirements focus on the essential capabilities of the drone and rover, ensuring they can perform their intended tasks accurately and reliably. This includes sensor systems that collect and process data, real-time communication protocols, and precise control mechanisms for both the drone's flight and the rover's movements. The system must ensure efficient operations, including solar panel cleaning, obstacle detection, and path optimization for the rover.

**Reliability & Fault Tolerance:** Reliability and fault tolerance are critical to maintaining continuous operation of the system. The requirements ensure that both sensor and communication systems operate without degradation over time, with the ability to handle errors autonomously. The system must also include recovery mechanisms for communication disruptions and include fault detection and handling protocols to ensure minimal impact on performance. The rover's autonomous navigation must ensure smooth and safe operation without failure.

**Power & Circuit Management:** The power and circuit management requirements ensure that the system receives stable and regulated power across all components, including sensors, motors, and control systems. The PCB components should support voltage regulation, signal filtering, and provide mechanisms for error handling. Power management also includes monitoring battery levels and managing power distribution for optimal system performance.

## 4. Final Design

This section presents the final design of the system, divided into two main parts: the drone design and the rover design, each addressing the key decisions involved in their development.

### 4.1. Drone Design

The following section details the drone design aspects of the final system, covering the motor and propeller selection, the release and capture mechanism, and the drone flight controller.

#### 4.1.1. Propeller and Motor Selection

Choosing the right motor and propeller was essential to make sure the drone could meet the required thrust-to-weight ratio. To select the motor, a benchmark analysis was done by comparing motors commonly used in similar-sized drones. Based on experimental datasheets found online, the GEPRC EM2812 900KV motor stood out since it provides high thrust with good efficiency, all at a reasonable cost, which made it the best fit for the design.

Once the motor was selected, the next step was to find a suitable propeller. Although the motor is typically rated for 7 to 9-inch propellers, the drone frame was large enough to allow for bigger propellers. So, both 9-inch and 10-inch propellers were tested to see which performed better. The 10-inch tri-blade propellers delivered more thrust during testing, which led to their selection for the final setup. The specifications for the motor and propeller are in Table 1.

*Table 1: Motor and Propeller Selection.*

Motor	GEPRC EM2812 900 KV Motors
Propeller	HQ Prop 10X5.5X3 Tri-blade

During the assembly of the drone's motor mounts onto the frame arms, only two out of the four bolt holes on the motor mount aligned with the corresponding holes on the carbon fiber arm. To assess whether securing the motor with only two bolts would be structurally adequate, a stress analysis was conducted. The critical stresses that were analyzed were the shear stress acting on the two M2.5 bolts securing the motors and the bearing stress acting on the motor mount. The equations used to evaluate these stresses are presented below:

#### Shear Stress:

$$\tau = \frac{F}{A}$$

Where  $\tau$  is the shear stress, F is the applied force, and A is the cross-sectional area.

#### Bearing Stress:

$$\sigma = \frac{F}{A}$$

Where  $\sigma$  is the bearing stress, F is the applied force, and A is the bearing area.

The analysis yielded margins of safety above 200, confirming that the two-bolt configuration would be sufficient to secure the motors under the expected loading conditions. This outcome eliminated the need for any design modifications. Had the margin of safety been significantly lower, the carbon fiber motor mount would have been replaced with a machined sheet metal version to accommodate all four bolts. However, given the favorable results, the decision was made to proceed with the two-bolt configuration.

#### 4.1.2. Release and Capture Mechanism

##### Structural Design

The component selection and specifications for the final design release mechanism remain the same as those described in the detailed design report. Additional specification was added to the fastening solutions on various components, particularly the electromagnets and frame arms, which required special consideration due to being key points of potential structural weakness in the design. Spacing and clearance considerations were also addressed by adding countersinks to holes on the bottom of the base plate and adding wire channels for the magnet wire routing. Adjustable friction-fit spacers were also added to prevent the entire base plate assembly from sliding laterally along the rod. These changes are shown visually in Figure 2 and Figure 3.

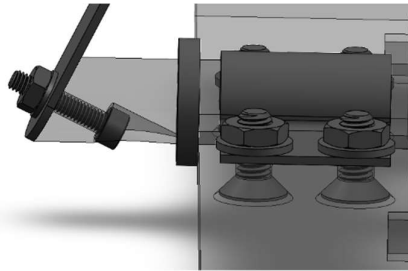


Figure 2: Release Mechanism, Counter-bored and Counter-sunk Fastener Holes.

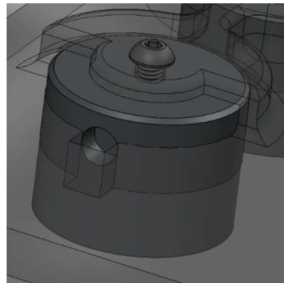


Figure 3: Release Mechanism, Magnet Fastening and Wire Channel.

A complete image of the final design CAD of the release mechanism is shown in Figure 4.

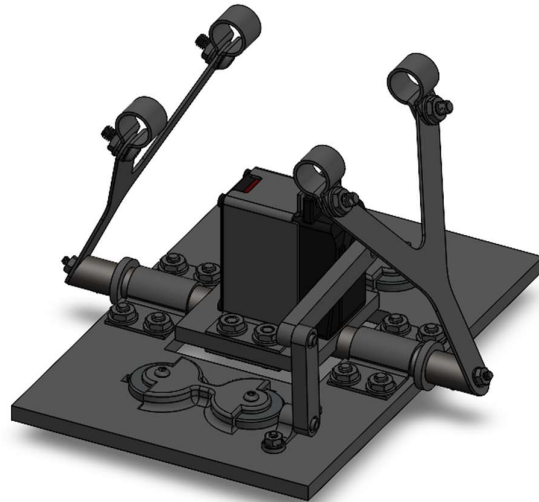


Figure 4: Release Mechanism Final Design CAD.

Note that the final design, which prioritizes scalable manufacturing and long-term reliability, makes the assumption of sheet-metal formed parts for many of the key structural elements. This contrasts with the manufactured prototype, which used 3D printed parts in all locations due to cost and time constraints. All deviations from this final design for purely manufacturing purposes are detailed in the Manufacturing Process section.

### Component Selection

Component selection for the release mechanism remains the same as the detailed design report – all analysis provided within still applies. A summary of the components selected, as well as the estimated design performance of the system, are provided in Table 2 and Table 3 respectively.

*Table 2: Release Mechanism Component Selection.*

Electromagnets	4x Uxcell 12V 25N lifting magnet
Servo Motor	Miuzei 20kg High-torque servo motor

*Table 3: Release Mechanism Final Design Specifications.*

Maximum Lifting Capacity	10kg
Peak rotational speed	112.5 deg/s
Deflection Range	0-25 degrees
Net Torque Output	30.78 kg cm
Mass	435.15 g

#### 4.1.3. Drone Flight Controller

The main controller used to fly the drone is an Xbox One Controller modified to fit the specific needs and uses for the SPCD project. While this controller allowed for directly functioning buttons, triggers and inputs, these inputs could not communicate by themselves with the flight controller installed on the drone. Therefore, to achieve this, two Arduinos components, one Uno installed on the controller and one Nano on the drone, allowed for two-way communication, using nRF24L01 antennas to propagate and receive the signals. Since several electronic components needed to be connected to the controller to allow it to perform its functions, an electronic box needed to be designed and printed to encase them.

As such, a box that could safely hold all these electronics to prevent them from dangling from the controller and being damaged was designed. It was also important for this box to have openings for the ports that would connect the controller to the electronics, as well as leave a space for the antenna to extend out of. Furthermore, making this box ergonomic meant that the person piloting the drone could hold the controller without being encumbered by sharp edges and corners. Lastly, this box would then be glued to the rear battery casing of the controller, which was the location that was the least restrictive ergonomics-wise.

The fully assembled and printed controller casing can be seen below. It is attached to the rear battery casing of the controller, which means that it does not interfere with the inputs from the operator. Note that there is an opening for the antenna at the top and two more openings for the ports used for connecting the controller to the Arduino as well as modifying the Arduino's code by connecting it to a computer. The top and bottom of the casing are secured using screws, which makes the box easy to open and close in case the inside components need to be modified.



*Figure 5: Controller with Fully Assembled Electronics Box.*

#### 4.1.4. Drone Structural Design

The drone frame was built from the purchasable Tarot Iron Man 690 Folding Carbon Fiber Hexacopter Frame due to its high payload capacity. Table 4 details the measured frame's specifications.

*Table 4: Drone Frame Specifications.*

Specification	Value	Unit	Notes
Center Frame Width	185	mm	
Arm Diameter	680	mm	Measured motor-to-motor
Propeller Clearance	340	mm	Adjacent motors distance
Payload Rods Distance	60	mm	Measured center-to-center
Payload Rods Length	280	mm	
Total Weight	577	g	Entire frame w/o landing gear

Even if the frame was not manufactured, it was still important to make a CAD of the model to visualize the entirety of the project before manufacturing it, to ensure accurate payload and propeller clearances, and to use it to make the design of any brackets that will be mounted on it, such as the battery brackets. Figure 6 shows the finalized model of the drone, equipped with the following (refer to Appendix E for a detailed drawing):

- 12 X 10-inch propellers (HQ Prop 10X5.5X3 Black glass fiber reinforced nylon)
- 6 X GEPRC EM2812 900KV Motor
- 2 X CNHL 6S Lipo Battery 10000mAh 22.2V 100C
- Other system components (see section 4.1.5).



*Figure 6. CAD Assembly of the Drone.*

Table 5 summarizes the flight mass budget of the drone:

*Table 5: Drone and Payload Mass Budget.*

Part Name	Mass Budget [kg]
Drone Frame	0.500
Drone System Components	3.500
Release Mechanism	0.500
Rover	1.500
Total	6.000

#### 4.1.5. Drone System Components

The drone's core control system consisted of an Arduino Nano, a radio module, a flight controller, and three electronic speed controllers (ESCs). The radio module received commands wirelessly from the ground controller, which were then processed by the Arduino. Acting as the communication bridge, the Arduino transferred these commands to the flight controller using the S-bus protocol. The flight controller interpreted these signals and issued motor control instructions to the ESCs. Each ESC was responsible for driving two motors, forming a compact and efficient flight control stack as shown in Figure 7.

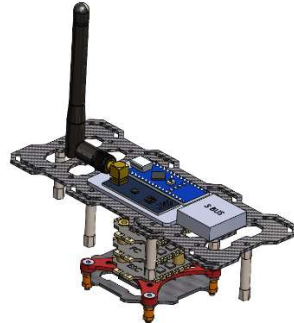


*Figure 7: Drone Stack and Electronics CAD.*

#### 4.1.6. Drone Landing Gear Design

Due to the requirements of the mission plan, which include a flight segment where attached landing gear is likely to collide with the solar panel mid-flight, an alternative solution for landing and take-off was necessary. For this purpose, the team designed a static landing platform, on which the drone could take off and land onto the drone arms instead. An image of the landing platform is shown in Figure 8. Dimensions were carefully chosen to fit all parts into the size of the printing beds available to the team. Engineering drawing of the assembly and individual components are available in Appendix F.

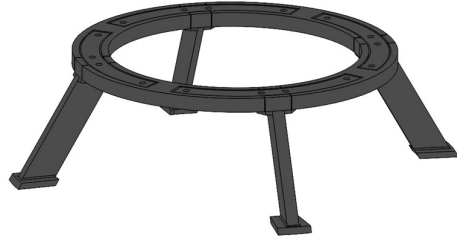


*Figure 8: Drone Landing Platform CAD.*

## 4.2. Rover Design

The following section outlines the finalized design of the cleaning rover, focusing on key elements such as the fuselage structure, track system, cleaning mechanism, and the integration of essential system components. Figure 9 shows the assembly CAD of the rover, while Figure 10 shows the detailed drawings.

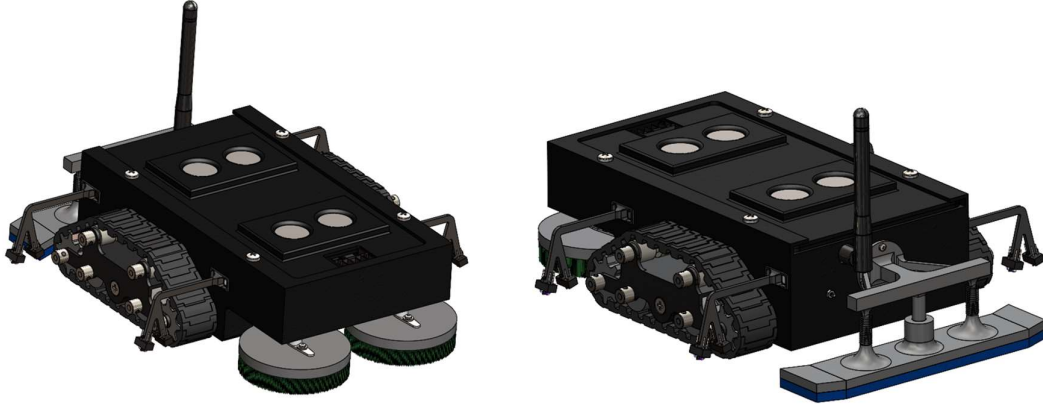


Figure 9: Rover Assembly CAD.

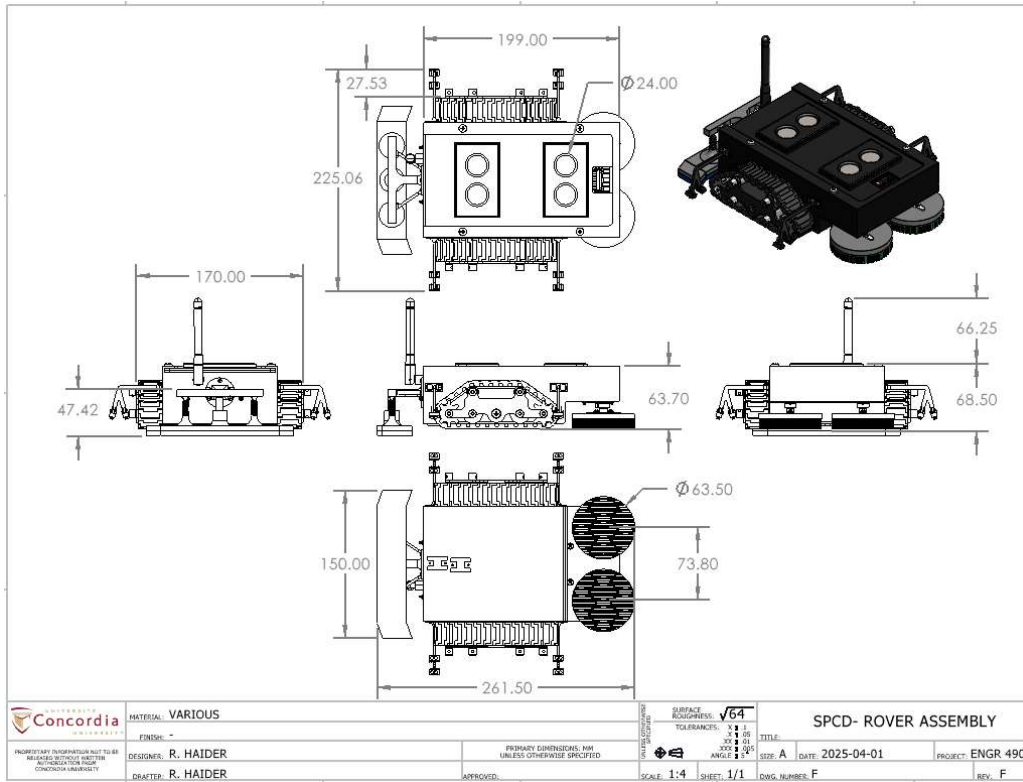
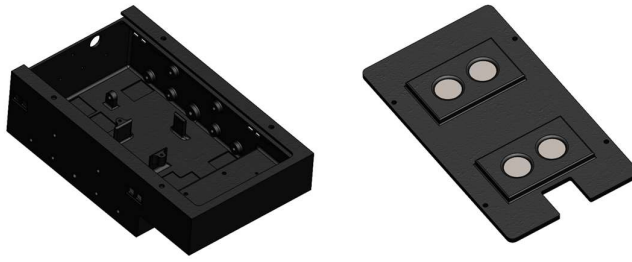


Figure 10: Detailed drawing of the rover

### 4.2.1. Rover Fuselage

As for the rover fuselage, it was designed to be as versatile as possible to account for any design changes that might happen in other components. It is composed of two main entities: the fuselage base and the fuselage cover, shown in Figure 11, both 3D printed with PLA. Detailed drawings are provided in Appendix G.



*Figure 11: Rover Fuselage and Cover CAD.*

The cover of the fuselage contained 2 magnetic metal sheets (22ga hot rolled steel sheet) that would be used for the release mechanism (see section 4.4). As mentioned, the fuselage was made flexible by adding extra bolt holes which could be used to mount extra system components that were not in the CAD. Additionally, the battery, motors and encoders were mounted onto the fuselage via printed brackets. Therefore, if those system components needed to be changed or displacement, only those brackets would have to be redesigned without needing to modify the fuselage. Those brackets are shown in Figure 12.

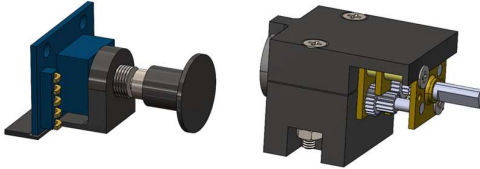


*Figure 12: Rover Wheel Encoder and Motor Brackets.*

#### 4.2.2. Track System

The displacement system was the most complex and critical component of the rover. Without a functioning system, the rover would not even begin the cleaning process, and the electrical components related to it, as well as any simulation, could not be properly tested. Therefore, very special and detailed attention were brought to its design, following the requirements shown in Table 6.

*Table 6: General Calculated Parameters for the Track System Sizing.*

Stress installation requirement on solar panels	2400.00 Pa [3]
Wheel friction force	16.62 N
Average rover speed	0.143 m/s
Cleaning time	13.62 mins
Turning radius	0 (differential turning)
Number of rollers/sprockets per track	4
Maximum length of tracks (chord wise)	0.12 m
Wheel diameter	0.016 m
Rubber track thickness	4 mm
Track width (spanwise)	0.0234 m
Torque requirement	2.05 kg-cm
Gear ratio	17/12
Motor	GA12-N20-12V100 [4]

Following those requirements, the appropriate pieces, such as the gears, the steel rods, the hex couplers, and more, were purchased to avoid any complex machining procedures. The design of the tracks was therefore driven by these purchased parts. Its design is provided in Figure 13, with detailed drawings in Appendix H.

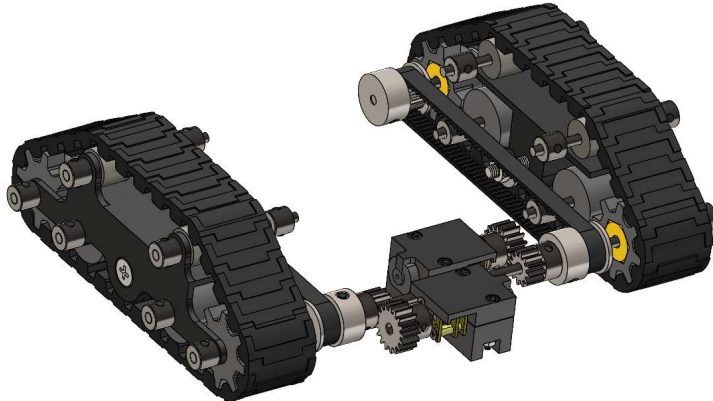


*Figure 13: CAD of the Rover Displacement System.*

Due to space constraints, the motors had no choice but to actuate the rear rollers, making a rear-wheel-drive vehicle. Additionally, it is common to have the driving motor at a  $90^\circ$  angle from the axis of rotation. However, due once again to volume limitations, the motors were aligned with the axis of rotation. The driven roller design is shown in Figure 14.

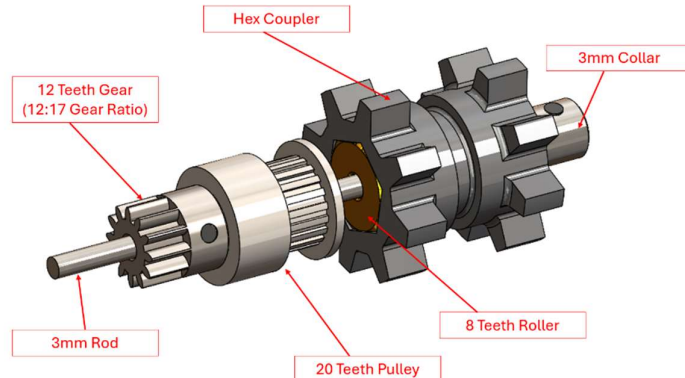


*Figure 14: Rover Driven Shaft CAD.*

The bracket assembly was designed to be rigidly linked to the body of the fuselage via an M4 bolt and 6 steel rods equipped with 2 set screw collars each. The minimal use of bolts came for the nature of the system itself; anything rotating had the chance to de-torque any bolts. As mentioned, the rear wheel was driven, and its movement was transmitted to the front rollers via a timing belt. 4 idle rollers (2 large and the bottom of the mounting bracket and 2 small on the top of the bracket) were also used.

For the track system, selecting suitable gears was essential to ensure that the components could safely withstand the torque applied during operation. The main objective was to verify that the bending stresses stayed within acceptable limits, maintaining a margin of safety above 2. A factor of safety of 2 was applied in the analysis to account for potential 2G loading scenarios, in line with common industry standards for stress analysis in mechanical components. The following equation was used for the stress calculation:

$$\sigma_b = \frac{W_t \cdot P_d}{F \cdot Y_j} \cdot K_s \cdot K_m$$

Where  $W_t$  is the tangential force,

$P_d$  is the diametral pitch,

$F$  is the face width,

$Y_j$  is the form factor,

$K_s$  is the size factor

And  $K_m$  is the load distribution factor.

After calculating the bending stress, the margin of safety was determined using the following equation:

$$MoS = \frac{\text{Allowable Stress}}{\text{Applied Stress}} - 1$$

The initial gear selection involved aluminum gears due to their lighter weight and lower cost. Using the motor torque values and gear geometry, the forces on the gear teeth were calculated, and the resulting bending stress was analyzed. However, the margin of safety came out below the target value of 2, making aluminum an unsuitable choice under the given load conditions.

To address this, the gear material was changed to steel, which offers significantly higher yield strength. With the same loading conditions, the switch to steel resulted in a much higher margin of safety, above the required threshold. While this decision increased both the weight and cost of the components, it was ultimately the better choice to ensure the system could handle operational stresses without failure. All gear parameters and bending stresses for both the driver and driven gears are presented in Table 7 and a comparison of both materials is represented in Table 8.

Table 7: Gear Bending Stress Calculation.

Parameters	Driver Gear	Driven Gear
Pitch Circle Diameter [m]	0.017	0.0125
Number of Teeth	34	25
Face Width [m]	0.005	0.005
Applied Torque [Nm]	1.57	2.13
Gear Ratio	1.36	1.36
Tangential Force [N]	251.14	341.55
Diametral Pitch [ $m^{-1}$ ]	2000	2000
Load Distribution Factor	1.25	-
Size Factor	1	-
Module of Gear	0.5	0.5
Tooth Form Factor	0.38	0.33
Bending Stress	264 MPa	300 MPa

Table 8: Comparison of Yield Strength and Margin of Safety for Aluminum Alloy and Steel.

	Aluminum Alloy Gears	Steel Gears
Yield Strength	270 MPa	1000 MPa
Minimum Margin of Safety	<0	2.33

#### 4.2.3. Cleaning System

After carefully reviewing the available cleaning methods, the final choice was to use rotating soft bristle brush at the front of the rover to remove dirt and bird droppings that could be stuck to the surface of the solar panel, followed by a microfiber cloth at the back of the rover to capture any remaining residue, to ensure a complete and effective cleaning procedure.

To rotate the brushes, the FM90 DC motor was chosen because it's light weight (8.4g) and good speed (around 110RPM). The brushes were sized so they could be slightly wider than the fuselage width, ensuring that they could cover the entire surface area of the solar panel as the rover moved across it, leaving no section of the panel uncleaned. Figure 15 shows the final designed assembly of the brush system, with the motor, the brush and the servo arm.

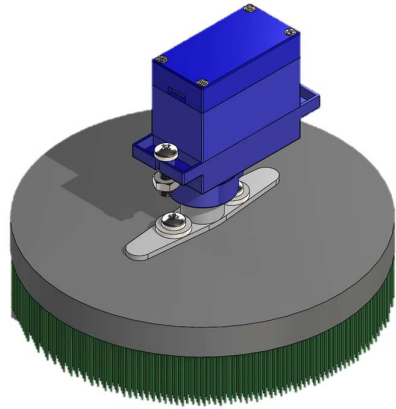


Figure 15: Final Brush System CAD.

A rod was developed to hold the microfiber cloth positioned at the back of the rover. The design included angled edges to more effectively capture remaining debris for a better cleaning. Figure 16 shows the final design. Figure 16 shows the first frozen design. Figure 16 shows the final design. A few modifications were made regarding this component during the manufacturing process, which will be discussed further in the report.

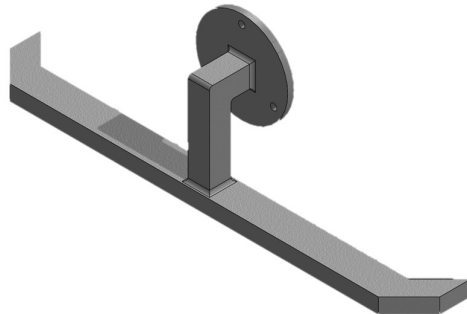


Figure 16: First Frozen Back Cloth CAD.

Detailed drawings with dimensions for the brush system can be found in Appendix I and the actual final design of the back cloth is shown in Appendix J (see section 4.5.3).

#### 4.2.4. Autonomous Control System

Due to hardware constraints, specifically the limited memory and processing capabilities of the onboard Arduino, we prioritized minimizing program size while maintaining a high level of reliability. To achieve this, the control system avoids using data-heavy or processing heavy sensors such as cameras. Instead, it relies on lightweight sensor inputs (e.g., IMUs and encoders) to support fully autonomous operation.

##### *Process Flow:*

The autonomous control system is structured around a predefined operational lifecycle, enabling the drone to execute its cleaning routine without human intervention. This process can be visualized on a high level in Figure 17.

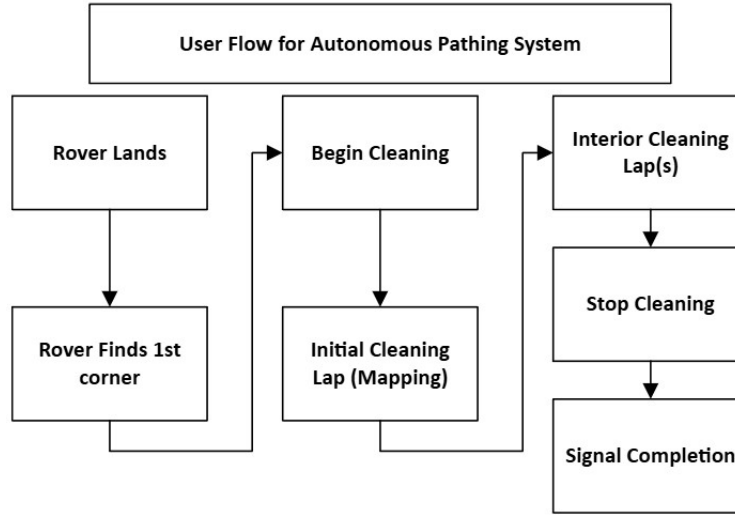


Figure 17: User Flow for Autonomous Rover Behavior.

The more detailed control logic follows the following sequence:

1. **Initialization:** The system remains in an idle state, awaiting an external start signal from the controller. This is to ensure that the rover starts operating after it has fully landed (avoid false starts)
2. **Navigation to Starting Point:** Upon activation, the drone navigates to the nearest corner of the solar panel array by utilizing the limit switches to first back up to an edge, align itself with it, then backing up until a corner.
3. **Edge Cleaning (Outer Loop):** It begins cleaning by tracing the perimeter of the panel array, ensuring all panel edges are cleared first. This step also ensures the rover can rely on its limit switches to validate IMU readings as well as record the surface width & length, providing a baseline to account for any initialization errors.
4. **Spiral Cleaning Path (Inner Loop):** After completing the outer loop, the system transitions into a spiral cleaning pattern, covering the central panel area efficiently. This method can then use the rovers cleaning area & the solar panel dimensions to clean the entire surface in a spiral pattern.
5. **Completion and Shutdown:** Upon completing the cleaning cycle, a stop signal is generated and sent to the controller, and the system returns to its idle state.

#### 4.2.5. Rover System Components

The following outlined the final design specifications for the rover's onboard systems. While changes were expected during the manufacturing phase, this configuration reflected the intended setup and rationale behind key component selections:

- **Arduino Nano:** Served as the main controller, coordinating all inputs and outputs across the system. The Nano was chosen for its simplicity of setup, compatibility with widely supported libraries, and the availability of both digital and analog pins.
- **Track Motors:** Were controlled by an L298N motor driver, which also provided a 5V output used to power the Arduino. The track motors were selected for their ability to deliver a good amount of torque while remaining small in physical size, allowing them to fit in the compact rover casing.
- **Limit Switches:** Were used for edge detection and connected through a multiplexer to reduce the number of required input pins (from 9 to 3), accommodating the Arduino Nano's pin limitations. These switches were chosen for their reliability, simplicity, and lightweight nature.
- **Cleaning Motor:** A counter-rotating brush motor was connected via a relay and powered through the 5V output from the L298N. This motor was selected after preliminary testing showed that 5V operation provided sufficient torque and brush force to effectively scrub the solar panel surface.
- **IMU:** Tracked the rover's orientation to enable inner-loop corrections and directional guidance. It was chosen specifically for its ability to provide reliable orientation data without requiring external references like GPS or vision systems.
- **Encoders:** Monitored wheel rotation to estimate speed and distance traveled. Their data, when combined with IMU readings, allowed for motion estimation and navigation across the solar panel.

The mentioned components are all shown in Figure 18.

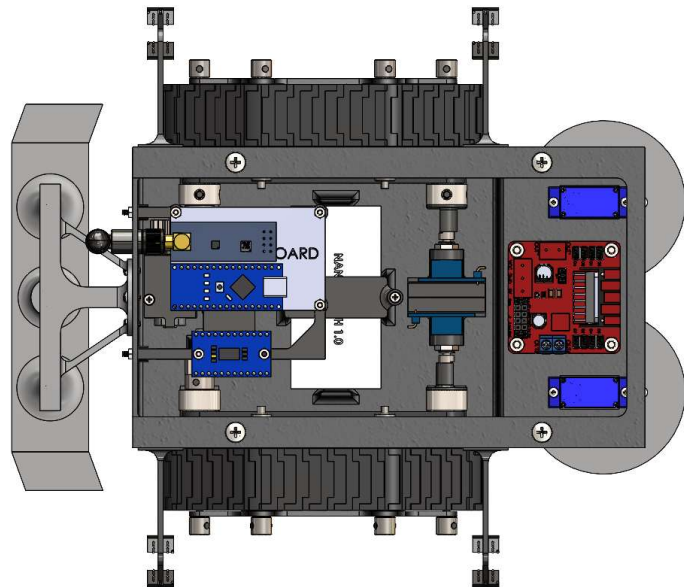


Figure 18. Rover System Components CAD.

The components above can be seen as a fully integrated system schematic for the rover in Appendix K. A similar schematic showing all drone systems is shown in Appendix L.

### 4.3. Drone Manufacturing

While the drone frame itself was purchased, several modifications had to be made to adjust it and be able to install the appropriate components and subsystems to it, such as the inclusion of the release and capture mechanisms as well as the drone stack.

Initially, the drone was shipped unassembled and design decisions had to be taken during its assembly. For instance, the drone usually is built with legs used as a landing gear. However, due to needing to drop off the rover on a slanted surface, the team opted out of installing this built-in landing gear and assembling the drone frame without it.

Furthermore, several components had to be fastened securely to this frame, namely the battery holders, the flight controller stack, and the electronics secured to the top plate. In most cases, to make integration simpler and more intuitive, the fasteners already present on the drone frame were used, however using longer lengths. For example, the flight controller stack was secured using an adapter plate that could use the same diameter bolts that were already connecting the frame's plates, which was more convenient. These electronics can be seen in Figure 19 below, with the red bracket being visibly fastened to the drone's lower plate using bolts.



Figure 19: Drone and Electronics Fully Assembled.

### 4.4. Release and Capture Mechanism

Contrary to the material assumption made in the final design section, which used a mix of printed and formed sheet-metal parts, the prototype release mechanism manufactured for demonstration and testing was made entirely out of 3D printed parts. For the parts that were previously formed sheet-metal, a deviation from the final design was necessary. This design change includes the removal of curves including bend-radius sections for brackets and fasteners, the addition of extra thickness to the now weaker critical structural components, and the addition of flanges to stabilize thin bracket sections. This required adjustment in the length and selection of fasteners.

Additionally, for the purposes of flight testing, the spacing brackets were modified to ensure the release mechanism would remain rotationally locked in flight. This is due to the team's decision to prioritize a successful flight test, rather than adding additional unknown variables that could impact the prototype drone's performance.

All parts were then assembled with machine screws, washers, and nuts, all of which are available parts purchased at Rona. After sanding and polishing to ensure proper tight or sliding fits for all contact-joints, the release mechanism was installed onto the drone payload bars. The complete assembly of the release mechanism prototype is shown in Figure 20.



*Figure 20: Assembled Release Mechanism.*

#### 4.4.1. Drone System Manufacturing

During the manufacturing phase of the drone, several changes and confirmations were made to the final design. As for components that aligned with the initial specifications, the motors were connected to electronic speed controllers (ESCs), which interfaced with the flight controller for stabilization and motor control. Command signals were successfully routed from the Arduino Nano to the flight controller, allowing higher-level autonomous functions to be coordinated. A radio module was integrated with the Arduino Nano to enable wireless communication with the ground control system; commands were relayed from the Nano to the flight controller (running Betaflight firmware), which then adjusted motor outputs via the ESCs. To secure the power system, a custom 3D-printed battery holder was fabricated, supplemented with velcro straps to keep the battery stable during flight. A buck converter was also installed to step down the battery voltage to 12V, providing power to the electromagnets used in the release mechanism. One of the key changes from the initial design necessary involved switching these electromagnets: instead of being driven directly by a digital output, the relay was triggered via a transistor circuit using a current-limited pin from the Arduino. This modification ensured actuation was possible while protecting the microcontroller from excessive current draw.

### 4.5. Rover Manufacturing

Once a semi-finalized design of the rover was accomplished, its manufacturing began to reveal any errors that could be present in the design. The main goal of the manufacturing process was to 3D print as much parts as possible. The fuselage was manufactured first, followed by the tracks and cleaning system. Finally, all the wiring required, and positioning systems were incorporated.

#### 4.5.1. Rover Fuselage

The fuselage was the first component printed from the rover, as shown in Figure 21. As mentioned, the design included extra holes to account for any unaccounted design changes. Most components attached onto the fuselage, such as the motors and encoders, were first mounted on printed brackets and glued or bolted to the fuselage. Therefore, if any design changes were made, only the design of the bracket would have to change without affecting the fuselage. Its design was therefore frozen after one successful PLA print.



Figure 21: Printed Rover Fuselage and Modifiable Brackets.

#### 4.5.2. Displacement System

Once the fuselage was printed, the displacement system was printed and assembled onto the fuselage, as shown in Figure 22. The designed mounting brackets are shown as mentioned in the previous section. As for the actual tracks, their manufacturing is detailed in section 4.7.

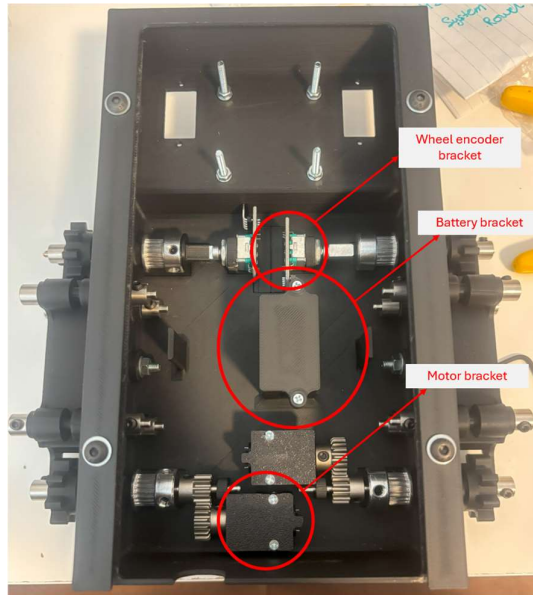


Figure 22: Physical Assembly of the Rover Displacement System.

As per the project's initial goal, components such as gears were purchased, and the rollers were 3D printed. The design was such that every single component would fit neatly within the purchased products, ensuring a quick and efficient assembly, avoiding the need of having complex metal machining procedures. The assembly could also be completely disassembled as needed, as long as the mounting brackets would not be glued to the fuselage. Only the following components needed some attention:

- Metal 3mm diameter rods: Needed to be cut with a Dremel.
- Timing belt: Needed to be cut and glued to the exact length.

As for the timing belt, its length needed to be exactly 230.2 mm, but this exact length was not available in the market. A belt strip therefore had to be sanded and glued together, but this process was very challenging and sensitive (see Figure 23). Therefore, a standard belt of 232 mm was purchased. While having a very slight sag, the belt still properly drives the rollers.



*Figure 23: Manufacturing Process of the Rover Timing Belts.*

#### 4.5.3. Cleaning System

For the brush system, the two brushes were purchased. Because they are meant to be cleaning surfaces while being attached to an electric drill, as shown in Figure 24, they had to be manufactured to fit into the fuselage. First, the metal part was removed using a hacksaw by cutting into the elevated part of the plastic. After cutting round it, the metal part was found to be super-glued to the plastic plate and was then easily removed. Then, the plastic plate was too thick compared to the designed one, was sanded using a belt sander, until the desired thickness was reached. Finally, the bristles, originally in a cone shape, were uniformly trimmed to the desired length, just enough so the bristles could effectively clean without scratching and damaging the surface of the solar panel. The final step involved integrating the brush system to the fuselage of the rover. The motors were mounted on the front part of the fuselage and secured using M2 bolts and nuts. The servo arm used to connect the brush to the motor was, first, super-glued to the surface of the plastic plate, then super-glued again to the motor arm. The final physical assembly is shown in Figure 25.



*Figure 24: Soft Bristle Brush, Before Manufacturing.*



*Figure 25: Final Physical Assembly of the Brush System.*

For the back cloth, multiple iterations were made, as mentioned in the final design section. The simplest way of manufacturing the rod was to 3D print it in one part. The first model, shown in Figure , broke when maneuvering the rover. An explanation for this failure would be that the vertical part connected to the base was too thin and the fillets were too small, resulting in insufficient surface contact with the base, causing it to break. To solve that issue, a second rod was designed and this time, the fillets were made a lot bigger and additional supports going from either sides of the vertical part were added, in an effort to increase the surface contact with the base, which was also longer, as shown in Figure 26.



*Figure 26: Second Design for the Back Cloth Rod.*

This design felt sturdier and overall better than the previous one, but the cloth wasn't fully compressed to the ground. The solution to make the rod even more effective was to design a third rod, shown in Figure 27 representing the final physical assembly, to incorporate springs that would compress the back cloth to the ground. The rod was divided into two parts, the top parts with 3 columns that would go into hollow cylinders from the bottom part when compressed. The overall height of the rod was increased as well, and the base was made wider and even longer to have a greater surface contact with the solar panel.

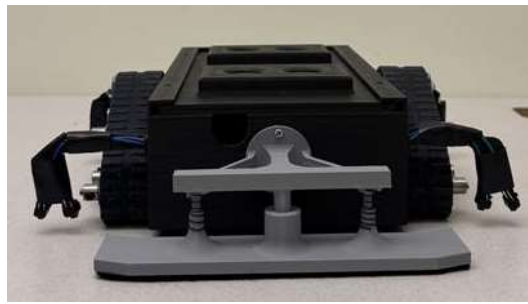


*Figure 27: Final Physical Assembly for the Back Cloth Rod.*

The final assembly of the back cloth was relatively simple. Using three M2 bolts and nuts, the rod was secured to the back of the fuselage, and the microfiber cloth was attached to the bottom of the base with Velcro, to facilitate the replacement of the cloth.

#### 4.5.4. Rover System Integration

During the manufacturing phase of the rover's onboard systems, several changes were made to the final design to address on the spot issues with sensors as well as performance improvements. The radio module was successfully connected to the Arduino Nano, preserving the intended communication pathway. For the limit switch system, a resistor array was added to ensure stable signal integrity; this involved a line of pull-down resistors and current limiters to protect the limit switches. Initially, a multiplexer was used to reduce the number of required Arduino pins, but testing revealed that it did not reliably pass the switch signals. As a result,

an ESP32 module was introduced in its place. The ESP32 handled all input processing for the limit switches and transmitted serial output to the Arduino, reducing both the pin count required and processing load on the Nano. Despite the addition of this second microcontroller, the ESP32's compact size ensured the rover remained well within its design weight constraints.

In terms of power distribution, the rover battery was initially routed through a buck converter to step down the nominal 14V to 12V, which was then fed into the L298N motor driver board. The L298N includes an onboard 5V regulator, which was originally used to power the Arduino and ESP modules. However, we later discovered that the cleaning motors were designed for 5V but could operate efficiently at slightly over 6V. With this increase in cleaning power, we added a secondary buck converter to step the voltage from 14V down to 6V specifically for the cleaning motors. This adjustment ensured that all components received adequate and stable power without overloading the motor driver board. All the wiring is shown in Figure 28.

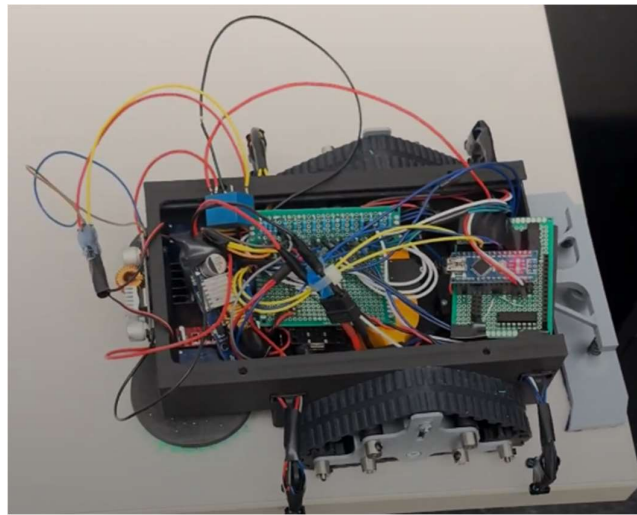


Figure 28: Rover Wiring for Testing.

#### 4.6. Design Validation and Testing

To validate the design, a flight test and a rover test were crucial for the success of the project. Two flight tests were performed, and the rover was also tested on a makeshift solar panel.

##### 4.6.1. Propeller Testing

Prior to performing any flight tests, validation of both the motors and propellers selected was necessary. The propeller testing was conducted at the Concordia Drone Lab, which provided the test stand and software required. Figure 29 shows the test stand and electronics used.



Figure 29: Propeller Testing Stand Assembly.

Results from the testing showed a small deviation in thrust between the published motor datasheet and the results obtained. However, these were likely due to a failure of the battery used in the experiment. After testing, the voltage on each individual cell of the battery was tested, and one cell read 1.5V (minimum safe LIPO cell voltage is  $\sim$ 3.0V) while the rest were in the expected range. It was concluded that this single-cell failure of the battery was likely a manufacturing defect, rather than being caused by any improper handling on the team's part. Despite the thrust results being impacted by the failed battery and the fact that only one battery would be available for the full flight test, the conclusion of the propeller testing was that, with the larger sized propellers, drone flight was definitively possible and would produce thrust within the expected range.

#### 4.6.2. Flight Tests

The initial flight test was performed on March 12, with the final design ready for testing. The drone used the manufactured circular landing platform as its landing gear, and a mock payload was used to simulate the weight of the rover without risking damaging it during the test. To this end, a barbell weight plate weighing 2 to 3 times that of the rover was strapped to the top cover of the rover, which allowed it to magnetically link to the capture and release system on the drone side. The PID controller for the drone flight controls were tuned as best as possible while lacking any physical data due to this being the first flight test.

At the start of the test, the throttle on the motors was progressively increased until the drone was able to lift off from the platform slightly. However, the payload rods on the bottom of the frame that were used to hold the capture and release system unfortunately got caught on the outer ring of the platform, causing the drone to tip and lose control, flipping upside down and knocking into the floor. While most of the drone was fortunately intact, one of the propellers' ends broke off after hitting the floor abruptly, which ended the test prematurely. The broken propeller can be seen in Figure 30 below.



Figure 30: Broken Propeller After Initial Flight Test.

After the failed initial test, due to not being able to test the drone's performance while hovering, a second test was planned. A replacement propeller was ordered and modifications to the PID were made to hopefully improve the stability of the drone. Furthermore, due to the landing platform being the main issue with the first test, it was ditched in favor of installing the legs that came with the drone frame. While this means we would not be able to simulate the exact conditions the drone would be flying in during an actual mission, the legs were deemed safer and more stable than risking the drone getting caught on the platform again.

The second flight test was performed on March 27, with the feedback and results explained above kept in mind. During this test, the drone was able to take off thanks to the fixed landing gear that was installed. It was able to hover for a few seconds before it was quickly landed to prevent it from losing stability. Noticeably, the drone had more than enough thrust to fly, but

stability was still not ideal, with the drone tipping slightly in one direction. Figure 31 shows the drone setup with the legs that came with the frame.



*Figure 31: Drone Assembly with Legs*

The key takeaways from these flight tests are the following. First, PID tuning and stability are critical for safe and stable flight, although confirming that the PID controller is properly tuned is difficult without access to more testing data. Second, the calculated thrust necessary for the drone to take flight with its payload was definitely overengineered, as takeoff and hover was achieved at around 30% of max throttle only. Therefore, focusing on stability may have been more important. Lastly, the height of the center of gravity of the drone frame was also noticed to be critical for stability. Due to the batteries resting on top of the frame and being the largest contributors to total weight, at over 1kg each for a total drone and payload weight of 6kg, the drone had issues with listing and not being generally stable. Lowering the center of gravity would have greatly improved stability, however there was not much space below the frame due to several components being there, like the capture & release system as well as the payload.

#### 4.6.3. Release Mechanism Testing (Aidan)

##### *Magnet Strength Test*

The strength of the electromagnets was evaluated using a small weight plate attached to the bottom of the rover cover. These results indicated that the magnet demonstrated the ability to easily attract the weighted plate onto the base of the rover and required significant additional force to remove. The results of this testing are shown in Table 9.

*Table 9: Magnet Strength Testing Results.*

Metric	Weight [kgf]
Maximum Demonstrated Pull Strength	2.33
Maximum Demonstrated Hold Strength	> 5.00
Design Pull Strength	1.5
Design Hold Strength	10
Required Pull Strength (Rover final weight)	1.1
Required Hold Strength	> 3.0

An image of the release mechanism successfully lifting the weighted plate shortly before the first flight test is shown in Figure 32.

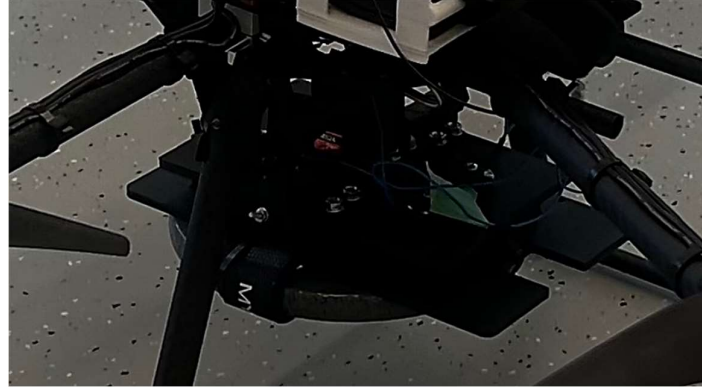


*Figure 32: Release Mechanism Weighted Test.*

Note that, while pull endurance tests were not performed, it was noticed that the magnets would get hot to the touch when powered on for over five minutes. This is likely to affect long-term holding strength of the magnet and may cause damage if the switching functionality fails.

#### *Switching Test*

During testing of the relay used to control the electromagnets in the release mechanism, it was initially attempted to switch the relay directly using a digital output pin from the Arduino Nano. However, this setup proved unreliable due to insufficient current drive from the pin, leading to inconsistent relay activation. To resolve this, the design was modified so that the digital pin instead triggered a transistor, which in turn switched the relay using the 5V power rail from the Arduino Nano.

#### *Servo Motors*

For validation and verification of the release mechanism, only tests on the magnets could be performed. The servomotor, which requires a 5V source above the current limitations of the drone Arduino, would need to be powered by an additional buck stepdown converter connected to the drone's main power source. However, since the team only acquired 3 buck stepdown converters, certain systems needed to be prioritized. Priority was given to the electromagnets and rover systems, and disassembly of these systems could not be performed in time for the servo motor tests to be conducted.

#### 4.6.4. Rover Testing

##### Simulation

To aid in the validation and testing of the rover design, a full-fledged simulation of the most relevant system components of the rover was performed. This was critical to allow for ongoing integration and implementation testing without having to rely on a physical working rover prototype platform. A component-by-component breakdown of modeling and testing activities is shown in this section.

##### Rover Motor Simulation

The rover motors were modelled using the following DC motor transfer function, in state-space representation, which relates the current applied to the motor to its rotation speed [5]:

$$\frac{d}{dt} \begin{bmatrix} i \\ \dot{\theta} \end{bmatrix} = \begin{bmatrix} -\frac{R}{L} & \frac{K}{L} \\ \frac{K}{J} & -\frac{b}{J} \end{bmatrix} \begin{bmatrix} i \\ \dot{\theta} \end{bmatrix} + \begin{bmatrix} \frac{1}{L} \\ 0 \end{bmatrix} V$$

Here, the constant  $K$  is the motor torque constant  $K_t = \tau/i$  taken from the track motor datasheet [6],  $J$  and  $b$  are the shaft inertia and viscous friction constants estimated through SolidWorks,  $R$  is the measured resistance of the DC motor, and  $L$  is the estimated inductance of the motor.

To adequately control these motors, a PID controller was implemented. However, due to the limitations of PID controllers only using error to determine output, and since the transfer function for the motors is well understood and easily verifiable, an additional feed-forward was added to the controller to allow the motors to more quickly reach steady-state. The PID control function is the following:

$$V_{out} = K_{ff}v_d + K_p E + K_i \sum(E\Delta t) + K_d \left( \frac{E}{\Delta t} \right)$$

Where  $v_d$  is the desired velocity and  $E$  is the error between the desired and current velocity. This generalized PID allows for the rapid response of well-understood stable systems while compensating for errors and nonlinearities present in the actual system. The tuned PID performance for step-input velocities using the modeled motor transfer function is shown in Figure 33.

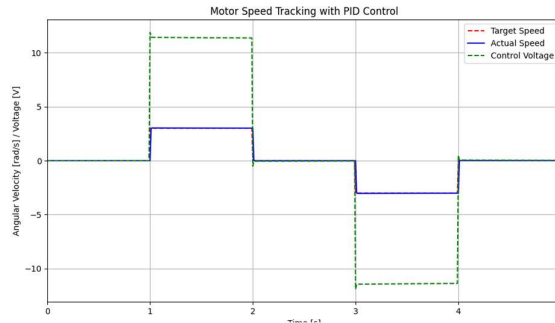


Figure 33: Rover Simulation - Motor Step Response and PID Tracking.

Additionally, simulating the dynamics of the rover's actual movement due to the motion of both tracks is necessary. The equations used to model this are the following:

$$V_{cg} = \frac{(\omega_l + \omega_r)r_{wheel}}{2}$$

$$\omega_{cg} = \frac{(\omega_r - \omega_l)r_{wheel}}{l_{axle}}$$

Conversely, this allows the desired left and right wheel rotation speeds to be set by specifying a desired forward velocity and rotation rate, as follows:

$$\omega_l = \frac{2V_{cg} - (l_{axle} \times \omega_{cg})}{r_{wheel}}$$

$$\omega_r = \frac{2V_{cg} + (l_{axle} \times \omega_{cg})}{r_{wheel}}$$

Control of the rover's direction and turning is then done exclusively through setting desired forward velocities and turn rates, or using higher-order methods (i.e., setting desired distance or heading) which then set desired forward velocity and turn rate. Desired left and right track velocities are then computed and controlled using the PID.

## Rover Sensing & Control Simulation

### *IMU*

Accurate modelling of IMU noise rates is critical to evaluate its real effectiveness in determining the position and orientation of the rover. The model applied used a Gaussian noise distribution with the noise rates given in datasheets to determine the measurement error of the IMU. Additionally, considerations for cross-axis coupling, drifting bias, and drifting basis vectors were included in the code, but physical component testing revealed this was not a large source of error. The noise model applied to accelerometer data is shown in Figure 34 below.

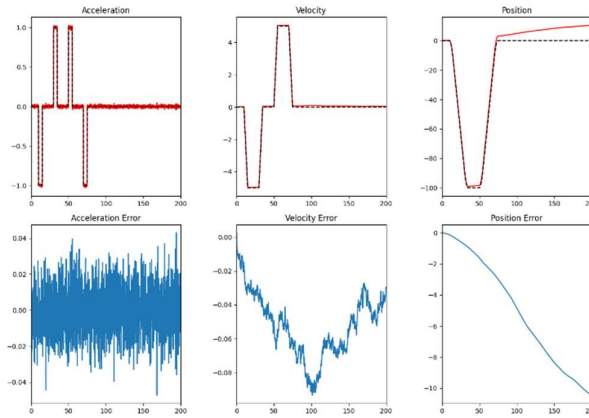


Figure 34: Rover Simulation - IMU Noise.

This data, especially regarding the error in position that the IMU accumulates over time due to double integration, lead to the decision of disregarding IMU accelerometer data and only relying on it for orientation, which proved to be much more accurate.

### *Encoders*

As position is no longer tracked through the IMU, finding an alternate means of determining position and velocity of the rover is critical. For this reason, the design includes rotary encoders attached to each track. These rotary encoders can serve a dual purpose, serving as measurement for the individual track PIDs and as a means of deriving the true velocity, position, and heading of the entire rover. However, due to the limited resolution available on the rotary encoders, simulated tests were required to determine whether the precision available was sufficient. Through testing, the following edge cases and compensation strategies were determined:

1. Due to the discrete nature of quadrature rotary encoders, if an encoder starts at a position very near one of the gates and immediately begins rotating and crosses a gate, the velocity reading will be much higher than the actual velocity. This also occurs if an encoder crosses a gate while transitioning from a positive to a negative velocity.
  - a. Ignore the first reading, and ignore readings in the opposite direction within a certain window
  - b. Add a buffer period where the rover is stationary and sensors continuously update
  - c. Add a short moving-average over the velocity readings
2. Since rotary encoders only provide readings every time they cross a discrete position, the encoder will continue providing the last returned velocity even while stopped.
  - a. Add a “zero time”, where if the time between readings reaches the zero time, the rover is assumed to be stopped, and the encoder returns a velocity of zero.

The performance of the rotary encoders to a simulated noisy velocity signal when adding these compensation methods is shown in Figure 35.

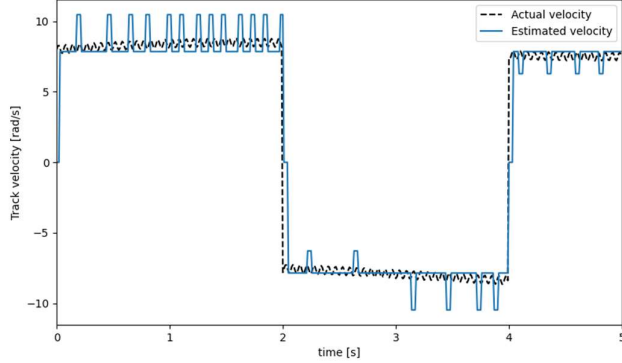


Figure 35: Rover Simulation – Encoders.

The results of feeding this sensor data into the track PIDs for a simulated constant rotation trajectory is shown in Figure 36 below.

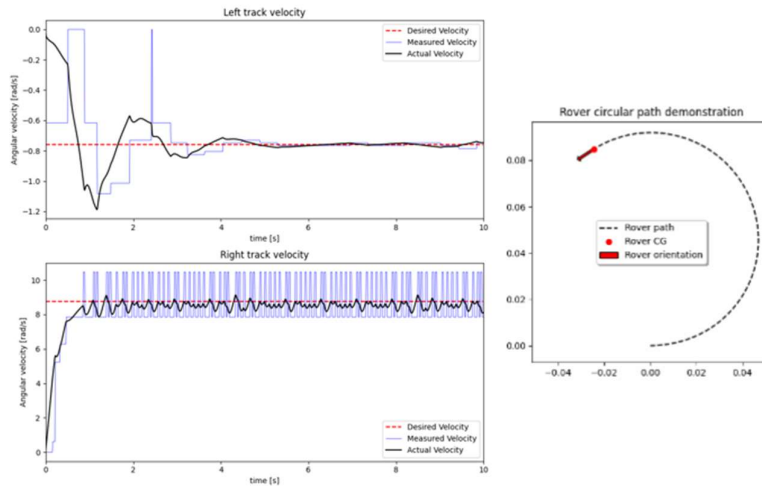


Figure 36: Rover Simulation - Track PIDs with Encoders.

These results indicated that the rotary encoders were sufficient for use in the PID control loop of the motors. However, as can be seen in the above graphs, the encoder error impacts the result much more strongly when the desired track velocity is relatively small. For this reason, further development will be focused on minimizing occurrences of low-velocity track movement.

#### *Position and Orientation PIDs*

Since the PIDs described above are only sufficient for setting and maintaining individual track velocities, and by extension rover velocity and turn rate, an additional layer of measurement and control must be used to allow the rover to rotate to a given fixed heading or move a certain distance along a straight line. The strategy selected is to use a cascaded PID setup to control the forward velocity and turn rate signals continuously while attempting to converge to a specific heading or forward distance. This approach compensates for positional or orientation drift during operation and leverages the stability of the already implemented track PID systems.

Additionally, since both small oscillations to converge to the desired setpoint and gradual low-velocity convergence are undesirable as these could amplify the effects of errors in the encoders and IMU, the rover will forcibly stop attempting to converge to a position or orientation when the measured value first exceeds the desired value. Graphical results of heading PID and distance PID tests are shown in Figure 37 and Figure 38.

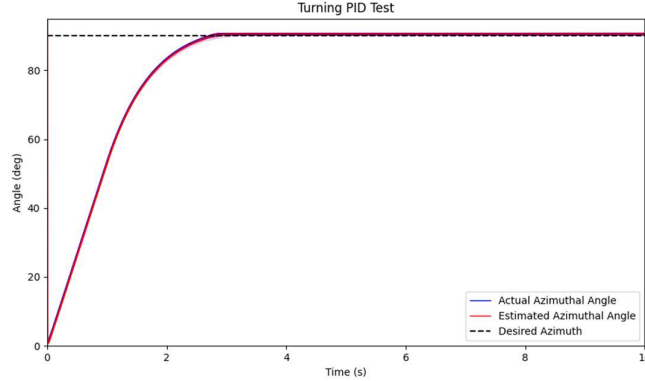


Figure 37: Rover Simulation - Orientation PID.

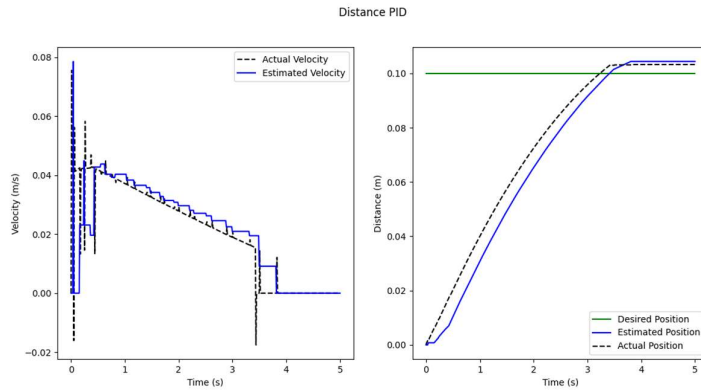


Figure 38: Rover Simulation - Positional PID.

### Limit Switches

The final sensor to be modeled is the limit switch. Its operation within the simulation is limited to a binary value, indicating whether the switch is currently within the bounds of the pre-configured simulated solar panel area. Limit switch positions are tracked based on their offset from the rover's CG, and their absolute positions are updated every timestep. Figure 39 shows an example of the limit switches identifying the edge of a simulated solar panel.

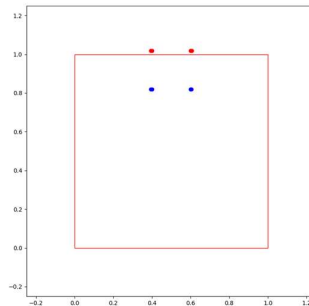


Figure 39: Rover Simulation - Limit Switches.

### Algorithm Testing

With the sensors and rover dynamics modelled, testing the soundness of the algorithm used to path and clean the solar panel is possible. After some fine-tuning and edge case handling, the simulated rover was able to follow the necessary algorithm to clean the simulated solar panel. Figure 40 shows a still image of the final state of the rover and the path it took to clean the solar panel, and Table 10 shows a breakdown of the time necessary to complete the mission, divided into the various mission segments.

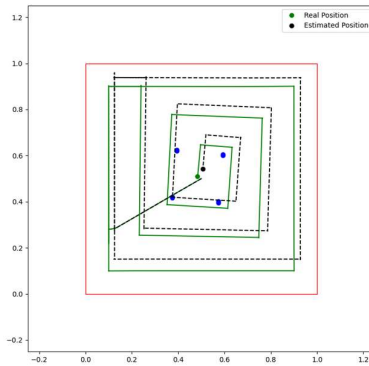


Figure 40: Rover Simulation Complete Mission Path.

Table 10: Rover Simulation Mission Time.

Segment	Time [s]
Search for Corner	36.96
Outer Loop	73.70
Inner Loop	68.42
Total	179.08

### Rover Physical Testing

A physical demonstration of the rover pathing algorithm was tested and performed in front of the course instructor. This demonstration included adjusted versions of the “Search for Corner” and “Outer Loop” pathing segments, as required due to deviations between the simulated and actual performance of the system. Since details and requirements of the test were demonstrated directly to the course instructor, this information will not be restated in this report.

#### 4.7. Design Deviation

After manufacturing the products and conducting some preliminary testing, a few problems in the design of the rover and drone were made apparent. Five major issues were noticed:

1. The rover tracks material was not meeting the requirements
2. One of the rover track motors was slipping and causing unreliable motion.
3. Replaced the limit switch multiplexer with an esp32 due to unreliable mux readings
4. Added an extra buck converter on the rover to get 5V output
5. The back cloth was not cleaning properly.

## Rover Track Material

As for the rover displacement system, the major issue occurred when manufacturing the tracks. An analysis conducted towards the beginning of the project showed that the tracks could be 3D printed with TPU, which would make it as versatile as possible. However, the TPU 85A purchased along with the design used for the tracks were extremely rigid, surpassing the 85A shore strength the product was rated for, as shown in Figure 41A. Therefore, the design underwent drastic weight and volume reduction but was still unable to fit the small bend radius the track rollers applied to it. As a last-minute solution, the team decided to mold the tracks out of liquid silicone with a shore strength of 30A, drastically reducing the rigidity of the tracks but considerably improving their flexibility. Although the material was believed to be too weak, the tracks turned out to have the perfect balance between elasticity and compressive resistance. The design is shown in Figure 41B and compared to the initial design in Figure 41C. It is evident that the initial design had a negative tendency to keep its circular shape.



Figure 41. Evolution of the Tracks, [A] TPU Tracks [B] Mold and Silicone Tracks [C] Comparison [D] Molding Process.

However, the material did come with its drawbacks, since the tracks were no longer tensioned properly to assure a uniform and undisturbed transmission of motion between the rear and front rollers. After a lot of research, a solution used in the locomotive industry was employed; the use of tensioner pulley, which is a manually adjusted wheel which alters the shape of the belt to adjust its tension. The best position to insert it was between the top rollers which had a lot of space between them. The final product, along with some design iterations, are shown in Figure 42. As shown, the height of the tracks was adjusted with a bolt and vertical slot.

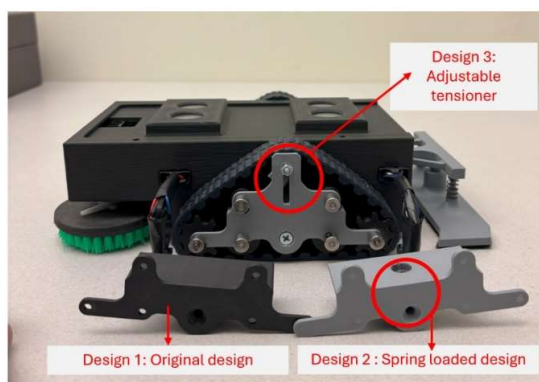


Figure 42. Design Iterations of The Rover Track Mount.

### Rover Track Motor

The Arduino implementation was adjusted to account for motor slippage by incorporating IMU feedback to detect deviations from straight-line movement. Despite these adjustments, the system continued to experience significant issues. Motor slippage led to performance degradation, causing the rover to either veer off course or fail to move altogether.

### Multiplexer Replacement Issue

The original multiplexer failed to reliably pass signals from the limit switches. As a result, it was replaced with an ESP32 module. This modification not only resolved the signal reliability issue but also introduced the benefit of localized processing. The ESP32 converted raw analog inputs from the switches into digitized signals using a dynamic thresholding method, thereby reducing computational load on the Arduino and improving input accuracy.

### Rover 5V Power Source

The L298N motor driver was unable to supply sufficient current at 5V for the brush motors. To address this, an additional buck converter was integrated into the system to step down the battery voltage to a stable 5V output, ensuring consistent power delivery for motor operation.

### Track Cleaning

The point 5 was addressed in section 4.2.3, so it will not be discussed in the following section.

## 4.8. Final Product

After all the design iterations, manufacturing and testing completed, the final prototype product was obtained. The final intended design of the drone is shown in Figure 43, and the final design for the rover on a solar panel is shown in Figure 44. The combination of both products is shown in Figure 45.



*Figure 43: Final Drone Model.*



Figure 44: Final Rover Model on Solar Panels.



Figure 45: Rover attached to the release mechanism (with the temporary landing gear legs).

To provide an accurate representation of the size of the rover, Figure 46 shows it on top of a rooftop solar panel.

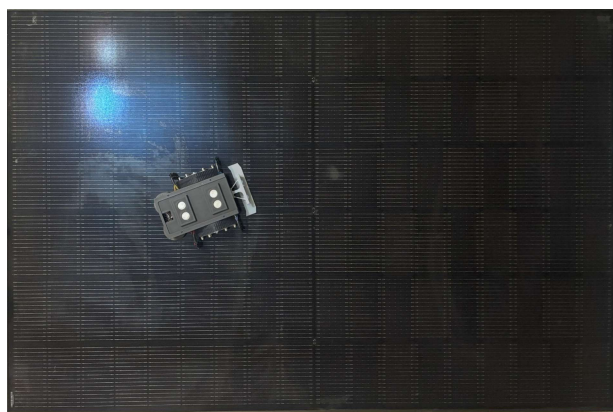


Figure 46: Rover On Top of Solar Panels.

Additionally, a comparison between the budgeted, designed and actual mass of the products are provided in Table 11. Contrary to the initial expectation, the actual mass of the entire product ended up being 2.10 kg lighter than the mass budget.

*Table 11. Mass Breakdown Of The SPCD.*

Component	Mass Budget [kg]	CAD Mass [kg]	Actual Mass [kg]
Drone	4.000	3.970	3.950
Landing Gear	3.000	2.150	1.590
Release Mechanism	0.500	0.406	0.390
Rover	1.500	1.251	1.030
*MTOW	6.000	5.627	5.370
Total Mass	9.000	7.777	6.960

\*Note: The Maximum Take-Off Weight (MTOW) does not include the mass of the landing gear

Finally, the SPCD team presented the project at the Capstone Design Presentation held on April 1st, marking the final stage of the project's development and showcasing the results of their collective efforts. Refer to Figure 47 for a picture taken during the presentation, featuring the final product.

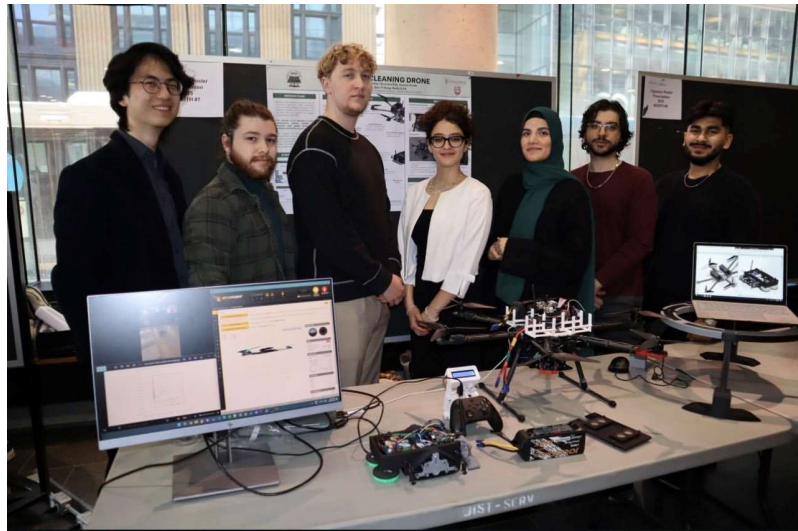


*Figure 47: SPCD Team Presenting the Final Product at the Capstone Design Presentation on April 1st.*

## 5. Cost Breakdown

The image below illustrates a well-known concept in software and systems development: the cost of change increases exponentially over time. Early in a project—during the Requirements and Analysis and Design phases—changes are relatively inexpensive. However, as the project progresses into Coding, Testing, and finally Production, the cost of making any modifications rises dramatically.

This concept directly ties into our drone and rover development project. Our design involved a wide range of integrated components across electronics, mechanical systems, and communication modules. By investing time early in the project to thoroughly plan, select, and simulate our components—such as the Tarot 690 Hexacopter Frame, MPU6050, Arduino Nano, and custom 3D-printed parts—we were able to catch design issues and integration challenges before moving too far along the curve shown in the graph.

That said, while we planned as much as possible ahead of time, we did run into some unexpected hiccups that required quick thinking and on-the-spot fixes. Fortunately, these issues were not central to our overall system design, meaning they were manageable and did not derail our goals. However, had they involved more critical components, the cost—both financially and in development time—could have been significantly higher. We did make some last-minute purchases to resolve these problems, which isn't ideal but was necessary to deliver the final system we had envisioned.

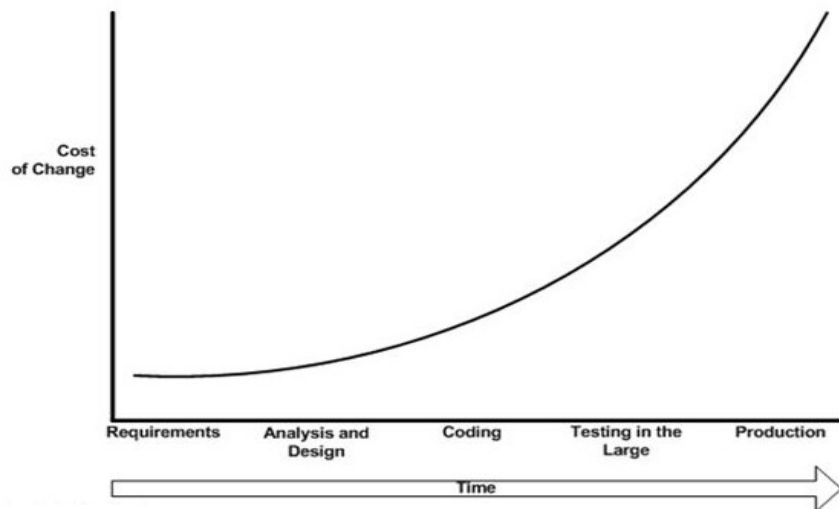


Figure 48: Cost of Change as Design Progresses.

The Table 12 to Table 14 and Figure 49 & Figure 50 below summarize our budget allocation for each system. While they offer a snapshot of spending, it's important to note that these overviews are supported by an in-depth itemized list of all components and materials used. This transparency not only ensured accurate budgeting but also allowed us to make informed decisions early—when changes were still affordable.

Table 12: Drone Cost Breakdown via Excel.

Drone		
	Category	Cost
Materials	Frame	226
	Propellers	35
Electronics	5v Buck Converter	4
	Battery	310
	Stack	245
	Communication	21
	Electro magnets	48
	Motors	233
	Servo	20
Testing	Smoke Stopper	9
	Fire Proof Bag	35
	EC5 Cables	
	LiPo Charger	50
Manufacturing	12 AWG wire	5
	Soldering Misc	70
	PLA Filament	50

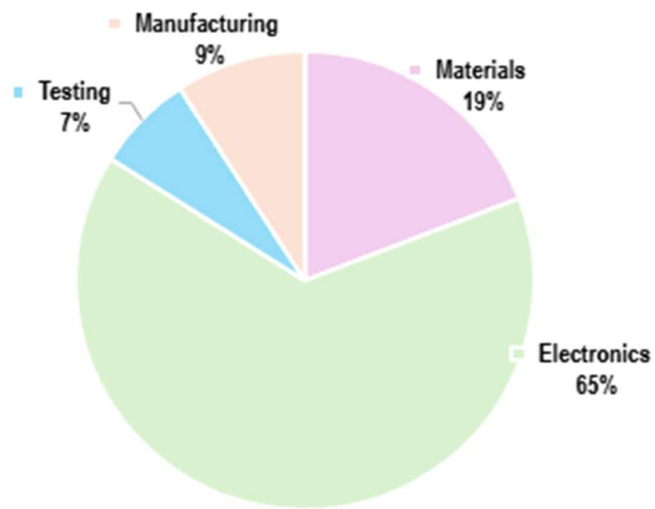


Figure 49: Drone Cost Breakdown Pie Chart.

Table 13: Rover Cost Breakdown via Excel.

Rover		
	Category	Cost
Electronics	Battery	39
	Track Motors	32
	Nano	6
	Limit Switches	10
	ESP32	6
	Cleaning DC motors	30
	5v Buck Converter	4
	L298N	10
	MPU 6050	15
	Wheel Encoders	18
Testing	Multimeter	Free
Manufacturing	TPU Filament	50
	PLA Filament	20

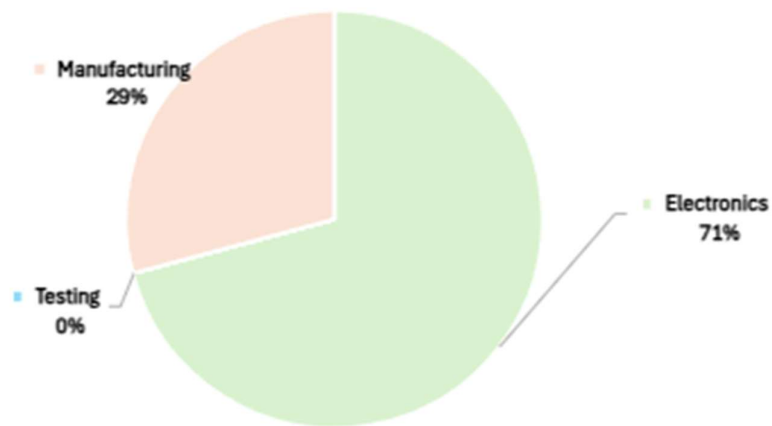


Figure 50: Rover Cost Breakdown Pie Chart.

Table 14 Expenses Excel.

Component	Price	Quantity	Purchase Date	Purchased By	Included	Total Price
Tarot 690 Hexacopter Frame	225.85	1	8-Nov	Nadim	<input checked="" type="checkbox"/>	225.85
6s 2x10000mAh Battery	310.42	1	20-Nov	Philip	<input checked="" type="checkbox"/>	310.42
Kakute H7V1.3 Stack	157	1	24-Nov	Philip	<input checked="" type="checkbox"/>	157
Tekkoh32 F4 4in1 50A ESC	88	1	24-Nov	Philip	<input checked="" type="checkbox"/>	88
arduino uno USB host shield	25.28	1	11-Oct	Philip	<input checked="" type="checkbox"/>	25.28
PWM to SBUS	15.43	1	25-Nov	Philip	<input checked="" type="checkbox"/>	15.43
arduino nano	6.02	2	9-Sep	Philip	<input checked="" type="checkbox"/>	12.04
5A DC-DC Step Down Buck	3.84	3	22-Nov	Philip	<input checked="" type="checkbox"/>	11.52
L298N Motor Module	5.2	2	25-Nov	Philip	<input checked="" type="checkbox"/>	10.4
NRF24L01	3.44	3	9-Sep	Philip	<input checked="" type="checkbox"/>	10.32
esp32-cam	9.78	1	11-Oct	Philip	<input type="checkbox"/>	9.78
Smoke Stopper 6s	8.99	1	24-Nov	Philip	<input checked="" type="checkbox"/>	8.99
atmega328p-pu	3.96	2	8-Sep	Philip	<input type="checkbox"/>	7.92
ICM-20948 IMU 9 axis	7.92	1	11-Oct	Philip	<input checked="" type="checkbox"/>	7.92
esp32 dev board	6.09	1	9-Sep	Philip	<input checked="" type="checkbox"/>	6.09
female header pins	13.88	1	23-Nov	Philip	<input checked="" type="checkbox"/>	13.88
12 AWG Wire	4.59	1	21-Nov	Philip	<input checked="" type="checkbox"/>	4.59
LCD IIC/I2C 1602	3.79	1	11-Oct	Philip	<input checked="" type="checkbox"/>	3.79
9v battery case	1.86	1	11-Oct	Philip	<input type="checkbox"/>	1.86
Soldering stuff (misc)	25.37	1	~	Philip	<input checked="" type="checkbox"/>	25.37
Import	78.48	1	24-Nov	Philip	<input checked="" type="checkbox"/>	78.48
Lipo Safe Bag + EC5 cable	34.24	1	~	Philip	<input checked="" type="checkbox"/>	34.24
Shipping	56.79	1		Philip	<input checked="" type="checkbox"/>	56.79
ABRA stuff	10	1	25-Jan	Philip	<input checked="" type="checkbox"/>	10
Amazon ec5 cables	32.18	1	26-Jan	Philip	<input checked="" type="checkbox"/>	32.18
PLA filament	55	1	~	Philip	<input checked="" type="checkbox"/>	55
GEPRC EM2812 900KV Motor	38.93	6	15-Dec	Oumaima	<input checked="" type="checkbox"/>	233.58
HQ Prop 10x5.5x3 + Gemfan Foldin prop F1051-3	40.44	1	28-Dec	Oumaima	<input checked="" type="checkbox"/>	40.44
Wheel Encoder	18.05	1	24-Jan	Raad	<input checked="" type="checkbox"/>	18.05
AMLESO 2pcs Rubber Track	13.59	1	5-Jan	Raad	<input checked="" type="checkbox"/>	13.59
Set Screw Collars (3mm Bore)	19.99	1	5-Jan	Raad	<input checked="" type="checkbox"/>	19.99
3mm Brass Hex Shaft	12.99	1	5-Jan	Raad	<input checked="" type="checkbox"/>	12.99
12T Gear	9.94	2	5-Jan	Raad	<input checked="" type="checkbox"/>	19.88
17T Gear	8.98	4	5-Jan	Raad	<input checked="" type="checkbox"/>	35.92
MECCANIXITY Pulley	10.79	2	5-Jan	Raad	<input checked="" type="checkbox"/>	21.58
MECCANIXITY Belt	10.99	2	5-Jan	Raad	<input checked="" type="checkbox"/>	21.98

## 6. Entrepreneurship and Logistics

The following section outlines key entrepreneurship and logistics considerations, including an overview of potential customers and investors, possible funding sources, market competitors, and an analysis of the product's life cycle.

### 6.1. Potential Customers and Investors

For initial commercialization, the solar panel cleaning drone would be marketed directly to professional solar panel cleaning companies such as Total Clean Team [7] and Premier Solar Cleaning [8]. These companies already provide large-scale cleaning services and could integrate the drone system into their existing operations to improve efficiency, reduce labor costs, and access hard-to-reach or high-risk installations more safely.

By adopting this technology, service providers would be able to offer a more consistent and automated cleaning process while minimizing downtime for clients. This approach also eliminates the need for individual solar panel owners to invest in or maintain their own cleaning equipment, making it an appealing, hassle-free option for both residential and commercial customers.

As the market for solar energy continues to grow, especially in regions with heavy dust or pollution, there's a rising demand for scalable and cost-effective cleaning solutions. The proposed drone system presents a compelling opportunity for investors focused on the renewable energy sector.

### 6.2. Funding Sources

During the development of this project, the SPCD team participated in an engineering design competition organized by Bell Textron, where they secured 1st place among other teams. This achievement not only demonstrated the project's technical strength and innovation but also led to an initial funding of \$650 awarded by Bell Textron to support the next stages of development. The team's participation at Bell Textron is illustrated in Figure 51.



Figure 51: The SPCD Team at Bell Textron.

Another potential source of funding for this project is the Gina Cody Innovation Fund, which supports student-led initiatives with strong commercialization potential. The fund offers a two-phase structure: in Phase 1, selected teams receive \$10,000 over three months to further develop their concept and explore market fit. Teams that progress to Phase 2 have the opportunity to pitch for up to \$50,000 over twelve months to build a functional prototype and begin engaging early users. This fund presents a valuable opportunity to secure financial support while gaining mentorship and entrepreneurial experience within the Concordia community.

### 6.3. IP and Patent Issues

While similar solar panel cleaning technologies already exist and some are protected by patents, this project focused on creating a more cost-effective and practical solution by combining a drone with an autonomous cleaning robot. Now that the design stage is complete, it would be important to conduct a thorough review of existing patents and relevant regulations to ensure there are no conflicts and to understand what requirements would apply if the product were to move toward commercialization.

### 6.4. Competitors

Current competitors such as Solar Drone [9] and DroneVolt [10] offer drone-based solar panel cleaning solutions that primarily rely on water hoses attached to hovering drones. While innovative, these systems often lack precision and can miss areas of the panels due to the challenges of maintaining stable flight and consistent coverage.

In contrast, the proposed system introduces a hybrid approach by combining aerial deployment with an autonomous cleaning robot that operates directly on the panel surface. This hybrid approach provides a more efficient cleaning performance while minimizing water usage and energy consumption.

### 6.5. Product Life-Cycle Analysis

The solar panel cleaning drone system would begin its life with a limited launch, potentially targeting early adopters such as mid-sized solar panel cleaning companies. The initial phase would focus on demonstrating the system effectiveness, collecting user feedback, and making any final adjustments to ensure reliability and ease of use in real-world conditions.

If the product becomes successful, it could enter a phase of growth, where demand expands and more companies integrate it into their operations. The system's affordability and reduced resource usage compared to traditional methods would make it an attractive option for companies aiming to improve efficiency and sustainability.

As the product gains widespread adoption, it would likely enter the maturity phase, where the focus would shift to enhancing durability, simplifying maintenance, or offering upgrades based on customer feedback. As competition increases, maintaining a competitive side in terms of cost-effectiveness and value would be essential to remain viable.

Eventually, as with any technology, the product may experience a decline if newer or more advanced solutions emerge or if market dynamics change. At that stage, support would likely shift to maintaining the system's functionality and addressing customer needs, while still considering future upgrades or replacements as technology progresses.

## 7. ELSEE Aspects

The ELSEE aspects refer to Ethical, Legal, Social, Economic, and Environmental considerations. These aspects needed to be considered throughout the project to ensure that the solution developed is responsible, sustainable, and acceptable to society.

Regarding the Ethical, Legal, Societal, Environmental, and Economical (ELSEE) implications of a Solar Panel Cleaning Drone (SPCD), there are several factors affecting the stakeholders. For instance, the solar panel cleaning companies this product is aimed to be marketed towards are concerned with having efficient cleaning without damaging the solar panels as well as reducing the risk of accidents and manual labor necessary. This is encompassed by the Ethical, Legal, and Societal implications. Furthermore, the proposed solution promotes renewable energy by optimizing solar panel efficiency, reducing dependency on fossil fuels, and lowering greenhouse gas emissions, all of which concern the Environmental aspect of the regulatory authorities involved in drone flight. Additionally, this project offers economic benefits by lowering operational costs for cleaning service providers and improving energy output for solar panel owners, impacting the Entrepreneurial aspect of ELSEE and concerning the sponsors and investors of the SPCD project, another of the stakeholders. It is known that improper operation or failure to adhere to safety guidelines could lead to potential issues with the technology, such as stability problems, damage to equipment or even interference with air traffic. That is why extra precautions are taken by carefully following all relevant regulations and implementing robust safety measures during development and testing. Table 15 below shows an overview of some stakeholders involved in this project ranked by importance:

*Table 15: ELSEE Stakeholders Overview.*

Ranking	Stakeholder	Description	ELSEE Aspect	Desired Features
1	Solar Panel Cleaning Companies	Primary client	Ethical Legal Societal	Efficient cleaning without damaging solar panels, reducing manual labor and risk of accidents
2	Regulatory Authorities	Oversee drone laws	Legal Societal Environmental	Legal compliance with aviation laws and ensuring public safety
3	Sponsors & Investors	Funding	Entrepreneurial Ethical	Profitable and sustainable project

When working with drones, it is important to take extra precautions and to follow all relevant laws and regulations during the development, testing and implementation phases of the project. It is known that improper operation or failure to adhere to safety guidelines could lead to potential issues with the technology, such as stability problems, damage to equipment or even interference with air traffic. A real-life involving a drone was identified and taken as a lesson by the team: The Gatwick Airport Incident. Multiple drones were spotted flying near the runway from December 19<sup>th</sup> to December 21<sup>st</sup>, 2018. Because they could cause a serious safety risk by colliding with aircraft during takeoff and landing, the Gatwick airport decided to suspend operations, leading to a significant disruption. Around 140,000 passengers and 1,000 flights were affected by that decision. Extensive measures were taken to address the situation by the police and the British Army but unfortunately, the drone operators were never identified. This incident was further analyzed using the ELSEE aspects. Ethically, flying drones in a restricted airspace endangered public safety. Legally, the operators violated the UK airspace regulations by flying drones near in a restricted area. Additionally, following the incident, the government expanded the no-fly zone for drones around airports from 1km to 5km and introduced mandatory drone registration and licensing for operators of drone over a certain

weight as well as tougher penalties for illegal use. Socially, as previously mentioned, the disruption affected around 140,000 passengers, causing fear and frustration. However, thanks to the media coverage, the news attention amplified social awareness of drone-related risks. Economically, the multiple flight cancellations and delays, along with passenger compensations and investments in anti-drone systems lead to an important financial loss for the airport. Environmentally, while the impact on that aspect was limited, increased fuel consumption from flight diversions may have contributed to additional emissions [11]. This incident further highlighted the importance of considering the ELSEE aspects into the team's drone design.

By observing current research and development (R&D) practices for companies involved in the same field as the SPCD project, it is possible to obtain further insight into the ELSEE aspects that are involved in such a project. For instance, two major competitors in the solar-panel cleaning sector that are involving drones in the cleaning process are Solar Drone [9] and DroneVolt [10]. From looking at these competitors, it is evident that certain recurring trends appear. For instance, both companies heavily insist on regulatory compliance, particularly following FAA and EASA laws and recommendations. Effectively, the Legal and Ethical aspects are the most critical for the SPCD project, as drone laws are very strict, and flying the drone in unsafe locations or conditions could result in serious safety risks. Researching the precautions and laws followed by already existing competitors in the market helped to that effect, allowing the SPCD project to move forward without infringing on any laws or regulations. Table 16 below shows an overview of the competitors and R&D trends followed by them.

*Table 16: R&D Trends with Competitors.*

Characteristics	Solar Drone	DroneVolt
Scale	International	International
Organization	Startup	Established Company
Resources	Crowdfunding	Stock Investors
Team Composition	2-10 employees	40+ employees
R&D Trends	Full Automation (Societal) Regulatory Compliance (Legal) Drone in Box System (Entrepreneurial)	Aerial Spraying (Environmental) FAA & EASA Compliance (Legal) Non-invasive Farmland Cleaning (Ethical)

To assure that the SPCD project is compliant with the ELSEE aspects, several steps were taken, whether concerning the design, manufacturing, assembly or testing. A good example of this compliance can be seen in the main manufacturing method used during this project: 3D printing. This manufacturing method was selected for its ELSEE compliance at the economical, environmental, and social levels. For instance, this manufacturing method is highly cost-effective for prototyping, making it more economically conscious than other alternatives such as sheet metal manufacturing. Additionally, the recyclability of the PLA material used for the filaments during 3D printing shows environmental compliance. Lastly, community involvement due to usage of the library's 3D printers shows a more social level of compliance for ELSEE aspects. An overview of some of the team's decisions as well as the ELSEE aspects that were aimed at with those decisions can be seen in Table 17.

Table 17: ELSEE Compliance Decisions.

Decision	ELSEE Aspect	Justification
Usage of LiPo batteries for power	Ethical Legal Environmental	<ul style="list-style-type: none"> <li>• Rechargeable, thus reducing waste</li> <li>• Proper storage in fireproof &amp; safe bags</li> <li>• Compliance with fire safety standards</li> </ul>
3D printing as main manufacturing method	Economical Environmental Social	<ul style="list-style-type: none"> <li>• Cost-effective prototyping</li> <li>• Recyclable on-demand manufacturing</li> <li>• Community involvement (library printers)</li> </ul>
Bursary awarded by an engineering company	Social Legal Economical	<ul style="list-style-type: none"> <li>• Financial support &amp; reduced project costs</li> <li>• Engineering company social engagement</li> <li>• Sponsorship awarded through the school</li> </ul>

As a justification for these design decisions that were aiming to comply with ELSEE, several sources have been found that further support these decisions. For instance, in Euro-Precision's article "Understanding Tolerances: What Every Engineer Should Know" [12], the author highlights how critical tolerance testing is in engineering, especially for more consumer-level manufacturing methods such as 3D printing. In fact, best practices in engineering include tolerancing every part in CAD drawings, ensuring that parts fit properly with the intended fasteners. Similarly, in the same vein for 3D printing tolerancing, LKprototype's article "Mastering 3D Printing Tolerances: Tips for Precision and Accuracy" [13], the importance of post-processing manufacturing techniques such as sanding and deburring is stressed. This is due to plastic being rigid but easy to sand after 3D printing is done, so these techniques are appropriate for improving the fit of parts and fasteners. From these sources, it is evident that detailed tolerance testing and sanding done by the team has greatly helped in obtaining a cleaner-looking final product with parts that fit well with each other, thereby complying with ELSEE's environmental and economical aspects. Figure 52 shows the 3D printing tolerance testing board printed by the team to test the filament's tolerancing with diameters for various standard bolt sizes:

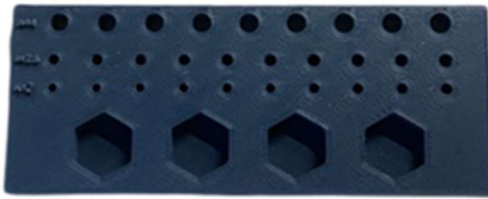


Figure 52: 3D Printing Tolerance Testing Board.

As the end of the project approached, the team reflected on the differences between the initial and final designs and identified some technical changes that were influenced by non-technical aspects, the first one being the motor selection for the propellers. Due to budget constraints, the team had to purchase motors with a lower performance than the ones initially chosen. A second change that was made throughout the project was the drone testing procedure. Initially, the flight test was scheduled to be in the Loyola Dome, where the drone could fly freely. Unfortunately, due to a storm, the dome collapsed, and, for legal and ethical reasons, the team could not fly the drone outside. A timeslot in a lab room was kindly offered to the team, but the procedure has to be changed because there was now a height limit of 2 meters that the drone could not exceed. Further reflection regarding ELSEE aspects prompted the team to think about risks as well as assumptions that were being taken in the project. A first risk regarding the social aspect was the noise pollution emitted from the drone, as it can be quite irritating,

especially in residential areas. During the propeller testing, it was clear that the propellers were loud and if the drone were to fly in a calm neighborhood, it would cause disturbance. A second risk regarding the ethical aspect were the safety concerns. If the project was to be implemented in real-life, people might be concerned about potential for malfunction or accidents. This could lead to fears about property damage, disruptions to daily life, or harm to individuals. A third and final risk regarding the economic aspect was the costly maintenance. During the development and testing phases of the project, the team took a risk by buying expensive motors and batteries without having a big enough budget or funding to re-purchase those items in case of malfunctioning. Looking into the assumptions, the first one was that the drone was complying with Canada's laws and regulations regarding drone use, since the team took necessary measures to make sure the scope of the project was legally acceptable. The second assumption was that the automation of the cleaning job will enhance efficiency rather than replace essential human jobs, which can be categorized in the ethical aspect. It was assumed that the system developed would complement the job by reducing risks of falls of injuries from rooftop work, expanding service coverage by allowing the cleaning companies to take on more jobs without increasing physical labor and by creating new jobs, like drone and rover operators and maintenance technicians. The third and final assumption was that the wildlife will not be disturbed, which is an environmental aspect. It relies on the idea that the drone and the rover will have minimal impact on the local wildlife, meaning the movement and presence of the drone in the air and the rover on the rooftop will not cause significant disruption to the animal behavior and nesting like birds and squirrels.

As future graduates, the team reflected on the important of ethics and societal considerations when designing an engineering product, the habits of thinking as a professional and the definition of a design failure. Engineering is not just about technical problem-solving, but also about creating solutions that safely and responsibly serve society. Ethics play a vital role in guiding design choices that affect communities and the environment. The final product should prioritize public safety, should be sustainable and respect laws and values of a society. Thinking as a professional engineer does require a strong technical knowledge, it also requires developing a mindset focused on responsibility and critical thinking. Just like a design should consider ethical considerations, an engineer should consider the safety and the ethics of a design by thinking critically and making data-driven decisions. The engineer should rely on evidence, simulations and real-life examples to guide a design, while ensuring that their work aligns with societal needs and professional standards. Finally, a design failure occurs when a product does not perform as intended, fails to meet user expectations, or creates risks for people or the environment. Economically, a design failure can lead to major financial losses and costly lawsuits. Legally, it may involve violations of laws, industry regulations, or safety standards, potentially leading to legal actions and business failure. Socially, a poor design can risk human lives, especially when safety is not properly prioritized. Environmentally, design failures can contribute to pollution, excessive waste, or long-term damage to ecosystems. Ethically, a design failure can happen when there is dishonesty, unfair treatment, or a lack of concern for how the product affects people. Overall, design failures highlight the importance of integrating technical accuracy with ethical responsibility and societal awareness in engineering work.

## 8. Safety and Risk Assessment

To better evaluate the impacts and concerns involved with the SPCD product on its shareholders and users, a list of possible risks that could compromise safety and health was drafted, as well as the likelihood and severity of each risk. For instance, a risk with a major impact on safety would be ranked higher and vice-versa. Similarly, the likelihood criterion represented how often a particular risk of failure would occur while testing or using the product. By accounting for both the impact level and likelihood of a risk, an overall severity level could be assigned to that risk. This severity level represents the overall seriousness of that risk, with higher severity risks being critical to the safety of the users and needing important mitigation plans.

To reduce the severity of these risks, a mitigation plan was also determined for each risk. The goal of these mitigation plans is to prevent the occurrence of these risks or to lessen the impact they have on the people involved as much as possible. For example, one possible risk that was determined is the electromagnetic capture and release system failing during flight. Due to it likely causing serious damage to the payload and/or drone as well as possibly affecting the operator or nearby crew, this risk was assigned an impact level of 5, which is the highest. On the other hand, this risk was only attributed a likelihood of 2 due to redundancy that was added to prevent this exact issue. In effect, the mitigation plan associated with this risk is magnet redundancy, resulting in a 2 sets of magnets per side rather than 1 per side.

The list of potential risks is shown in Figure 53 below, as well as the severity grid for each risk being shown individually in the rating grids below the main table as well, as seen below:

Risk ID	Description	Impacts	Likelihood	Severity	Mitigation Plan
1	Electromagnetic capture/release system failure	5	2	High	Magnet redundancy (2 sets of magnets per side)
2	Rover navigation & positioning error propagation	2	4	Med	Edge detection to prevent rover from falling
3	Project budgeting issues	1	3	Low	Bell projects competition bursary
4	Electronics/power distribution issues	4	3	Med	Battery redundancy and solder board testing
5	Insufficient thrust-to-weight ratio	3	1	Low	Six-motor configuration and weight safety factor

Figure 53: Risk Assessment List and Mitigation Plans.

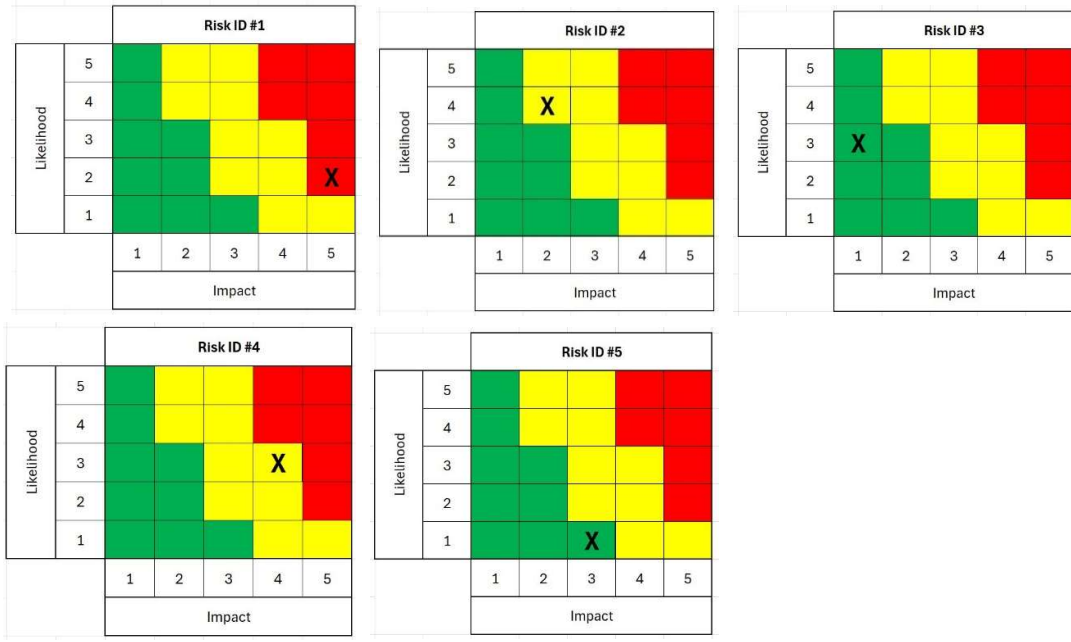


Figure 54: Risk Severity Grids.

In addition to the risk assessment, a Functional Hazard Assessment (FHA) was conducted to identify potential hazards caused by functions and their impacts on the system's functionality. To do so, a list of critical elements was listed for both the drone and the rover as well as their respective function. Then, these functions were assessed to identify failure modes and their effects on the system. Finally, each function is classified according to their level of severity. The classification went as follow, from the least severe to most severe: no safety effect, minor, major, hazardous, catastrophic. For example, in the case of the drone, the magnets were the first element analyzed. Their function was to hold the rover during the flight stage of the operation. The failure mode identified was that the magnets deactivated prematurely, leading to the rover falling mid-flight. This effect was classified as catastrophic, since it would lead to the rover being dropped from a significant height, resulting in complete loss of the rover.

The complete FHA for both the drone and the rover can be found in Table 18 and Table 19 respectively.

Table 18: FHA for the Drone.

Element	Function	Failure Condition	Effect of Failure	Classification
Magnets	Holds the rover during the flight stage	Magnets deactivate prematurely	Rover falls mid-flight	Catastrophic
Motors for props	Allow props to rotate, providing lift	Loss of motor power for all props	No more lift and drone crashes	Catastrophic
		Loss of motor power for one prop	Drone loses control	Hazardous
Batteries	Distribute power to all systems on the drone	Batteries fail	Complete power loss	Catastrophic
Release Mechanism	Rotates to release the rover at an angle	Mechanism fails to rotate the rover	Rover drops on the solar panel and damages its surface	Severe
GPS signal	Navigation	Loss of GPS signal	Drone loses position	Major
RC Controller	Allows pilot to control the drone	Loss of remote control	Drone crashes	Catastrophic

Table 19: FHA for the Rover.

Element	Function	Failure Condition	Effect of Failure	Classification
Track System	Allows rover to move around the solar panel	Motor fails	Rover stops moving	Major
		Wheel encoder fails	Rover stops moving	Major
Edge Detection Sensors	Detects edges	Sensors fails to detect an edge	Rover falls off the panel	Catastrophic
		“False positive” detection of an edge	Rover stops/turns without cleaning	Minor
Cleaning Brushes	Cleans the surface of solar panel	One motor stops working	Decrease of cleaning efficiency	Minor
		Both motors stop working	No more cleaning	Major
Batteries	Provides power to all systems on the rover	Batteries fail	Total loss of power and rover stops working	Major

## 9. Lessons Learned

Throughout all the phases of the project, the team encountered multiple challenges that redefined the scope of the project. Key lessons included the importance of subsystem validation, material testing, redundancy in critical systems, and adaptability in response to unplanned issues. The project demonstrated the need to align theoretical design with real-world performance and emphasized the value of iterative development in engineering design.

The initial goal of the project was to design and manufacture the entirety of the project and make the entire system autonomous. However, due to budget, time and knowledge constraints, the scope of the project was redefined to make it simpler, allowing us to purchase some components, such as the drone frame, while focusing the team's resources on more critical components, as shown in Figure 55.

However, the team's initial guess on the complexity and size of the project was very different from the final product, going from a small quadcopter to a very robust hexacopter design.

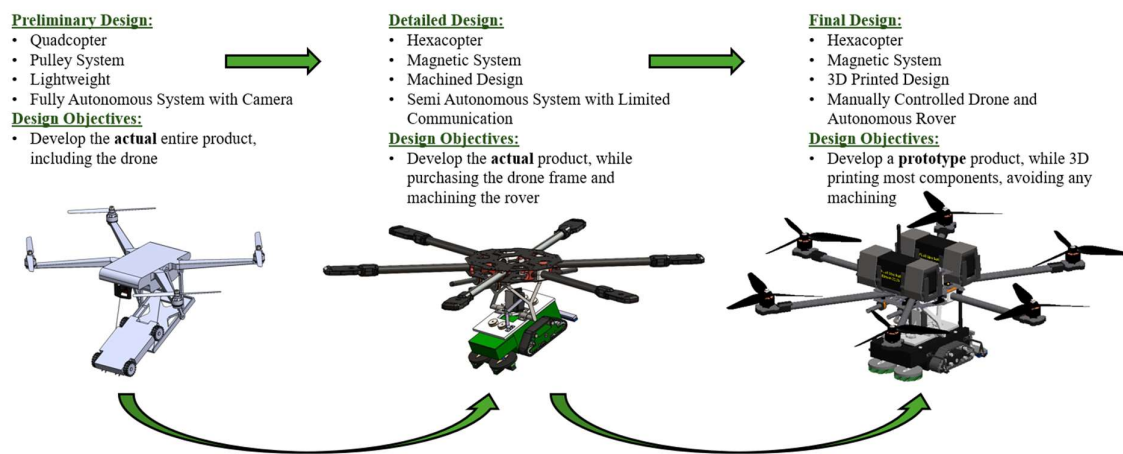


Figure 55. Scope and Design Evolution of the SPCD Project.

If the project were to be re-done, the main and most impactful change the team would have performed would be to properly define the scope and goal of the project and differentiate it from the mission plan. Rather than trying to design an actual marketable product, it would have been better to start the project aiming to design a prototype, which would have allowed the team to better allocate the resources to more critical components of the project.

The next steps of the SPCD project would be to develop a marketable and sellable product with all the notions learned during the last 8 months.

## 10. Conclusion

The Solar Panel Cleaning Drone (SPCD) project aimed to develop a semi-autonomous system for cleaning rooftop solar panels using a drone and a ground-based rover. The system was designed to improve safety and accessibility while maintaining cost and environmental considerations.

The final implementation met key functional objectives. The drone subsystem integrated a flight controller, ESCs, and a release mechanism, with communication managed through an Arduino and radio module. The rover incorporated a differential track system, cleaning mechanism, and onboard sensing for navigation and panel detection. Component testing and validation highlighted several challenges. Motor slippage in the rover and stability issues in the drone required iterative tuning. The use of silicone-molded tracks and a revised sensing architecture using an ESP32 improved system reliability.

Design deviations were made based on test outcomes and hardware limitations. Manufacturing was constrained by time and budget, leading to the use of 3D-printed components in the prototype. Safety and regulatory considerations were incorporated through a hazard assessment and review of drone operation laws.

## References

- [1] Precedence Research, "Rooftop Solar Photovoltaic Market Size, Share, and Trends 2024 to 2034," September 2023. [Online]. Available: <https://www.precedenceresearch.com/rooftop-solar-photovoltaic-market>. [Accessed 02 08 2024].
- [2] Aurora, "Understanding PV System Losses, Part 3: Soiling, Snow, System Degradation," [Online]. Available: <https://aurorasolar.com/blog/understanding-pv-system-losses-part-3-soiling-snow-system-degradation/#:~:text=Soiling%20loss%20is%20when%20dust,of%20calculating%20PV%20system%20losses..> [Accessed 02 08 2024].
- [3] H. Li, "Analysis of Deformation and Strength of Solar Module Support under Wind-Wave Load," 29 April 2015. [Online]. Available: <https://www.atlantis-press.com/proceedings/icmse-15/25845821>. [Accessed October 2024].
- [4] ABRA Electronics Corp., "12V 100RPM Mini DC Motor with Metal Gears - GA12-N20 Series," ABRA Electronics Corp., 2004. [Online]. Available: <https://abra-electronics.com/electromechanical/motors/gear-motors/mini-metal-garmotors/ga12-n20-12v100.html>. [Accessed October 2024].
- [5] MATLAB, ""DC Motor Positioning: System Modeling",," [Online]. Available: <https://ctms.engin.umich.edu/CTMS/index.php?example=MotorPosition&section=SystemModeling>. [Accessed 13 March 2024].
- [6] ABRA, "12V 100RPM Mini DC Motor with Metal Gears - GA12-N20 Series," [Online]. Available: <https://abra-electronics.com/electromechanical/motors/gear-motors/mini-metal-garmotors/ga12-n20-12v100.html>. [Accessed 13 April 2025].
- [7] Total Clean Team Inc, "Solar Panels Cleaning," [Online]. Available: <https://www.totalcleanteam.ca/solar-panels-cleaning/>. [Accessed 11 09 2024].
- [8] "Premier Solar Cleaning," [Online]. Available: <https://premiersolarcleaning.com/>.
- [9] "Solar Drone," Solar Drone, 2022. [Online]. Available: <https://www.solardrones.net/our-technology/>. [Accessed 22 September 2024].
- [10] "DroneVolt," DroneVolt, 2024. [Online]. Available: <https://www.dronevolt.com/en/>. [Accessed 22 September 2024].
- [11] S. Shackle, "The Guardian," 01 December 2020. [Online]. Available: <https://www.theguardian.com/uk-news/2020/dec/01/the-mystery-of-the-gatwick-drone>. [Accessed 10 April 2025].
- [12] F. Mughal, "Understanding Tolerances: What Every Engineer Should Know," Euro-Precision, 12 11 2024. [Online]. Available: <https://www.euro-precision.co.uk/post/understanding-tolerances-what-every-engineer-should-know>. [Accessed 13 4 2025].
- [13] LKprototype, "Mastering 3D Printing Tolerances: Tips for Precision and Accuracy," LKprototype, 27 3 2025. [Online]. Available: <https://lkprototype.com/3d-printing-tolerances/>. [Accessed 13 4 2025].

## Appendix A

### Team Breakdown Structure

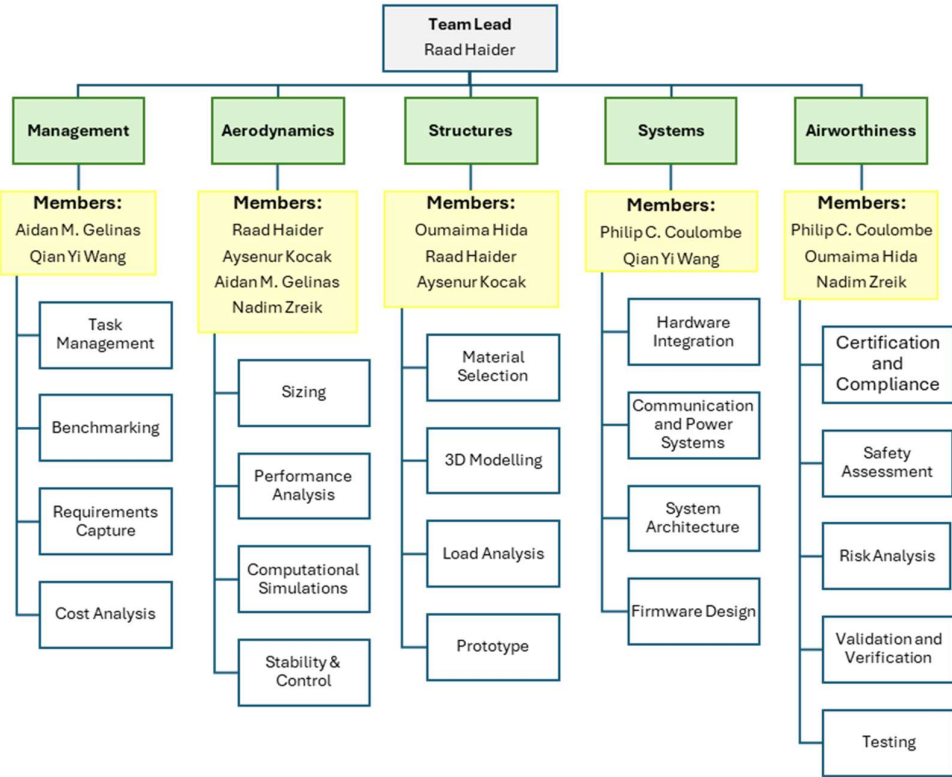


Figure 56. Team Breakdown Structure.

## Appendix A contd.

### Work Breakdown Structure

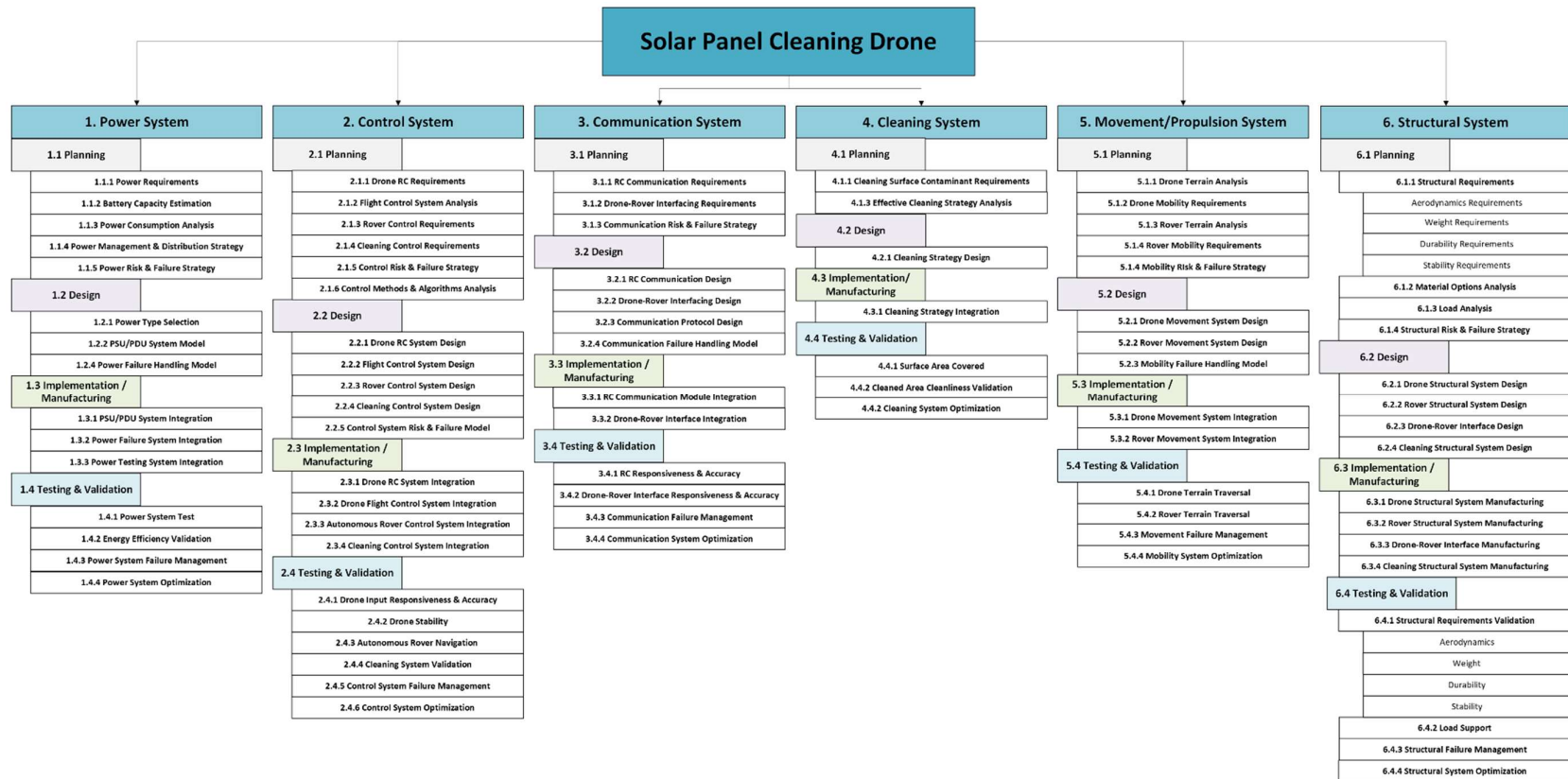


Figure 57. Work Breakdown Structure.

## Appendix B

### Breakdown of the Main Requirements for All Subsystems

*Table 20: Breakdown of Main Requirements for All Subsystems.*

Category	ID #	Topic	Requirement text	Related function
CANADA'S LAWS	1	Transport Canada requirement	The drone shall be registered with Transport Canada and marked with a registration number that must be clearly visible.	Drone registration and identification
	2	Transport Canada requirement	The pilot/person controlling the drone shall get their drone pilot certificate from Transport Canada that must be carried at all times.	Operator certification
	3	Authorized airspace	The drone shall fly at an altitude below 122m/400ft.	Maximum altitude
	4	Safety	The drone shall fly away from bystanders, at a minimum horizontal distance of 30 meters (basic operations) and never over them.	Bystander safety and distance control
	5	Authorized airspace	The drone shall not fly near sites for emergency operations or special events (avoid forest fires, outdoor concerts and parades)	Restricted navigation
	6	Authorized airspace	The drone shall not fly within 3 nautical miles (5.6km) of an airport or 1 nautical mile (1.9km) of a heliport.	Restricted navigation
	7	Authorized airspace	The operator shall fly the drone only in uncontrolled airspace (basic operations) while maintaining a visual line-of-sight with the drone.	Visual monitoring
	8	Lights	The drone shall be equipped with lights if flown during the night.	Operation at night
	10	Operation and protection	The pilot shall respect the privacy of others while flying and fly far away from other aircraft.	Privacy and safety
	11	Drone frame weight	The drone frame shall weigh 577g	Weight limit
WEIGHT	12	Rover fuselage weight	The rover shall weigh no more than 1500g.	Weight limit
	13	Cleaning system weight	The cleaning system shall weigh 71g	Weight limit
	14	Release mechanism weight	The release mechanism shall weigh 433g	Weight limit
	15	Traction system weight	The traction system shall weigh 154g	Weight limit
	16	Components	The cleaning rover shall be equipped with two brushes in the front and a microfiber cloth at the back to clean the surface of the solar panels.	Cleaning system components
CLEANING SYSTEM	17	Cleaning performance	The cleaning rover shall be capable of effectively removing dust, bird droppings, and leaves from solar panel surfaces to ensure optimal performance without damaging the surface of the panels	Debris removal
	18	Motor performance	The motors shall be capable of rotating the brushes at 100rpm.	Motor performance
	19	Operation	The cleaning rover shall autonomously navigate on the solar panels using sensors to build a map of its trajectory.	Autonomous navigation

TRACTION SYSTEM	20	Equipment	The traction system shall be equipped of rubber tracks and wheels to smoothly move the rover on the solar panel surface	Movement system
	21		The traction system shall carry the rover's weight without slipping at maximum angles of 25°	Provide grip
	22	Operation	The rover shall be able to clean an arrangement of 8 panels in 13 minutes	Cleaning time
	23	Panel safety	The system should distribute the rover's weight evenly across the tracks to prevent concentrated pressure on any single point of the solar panel, avoiding damage.	Weight distribution
RELEASE MECHANISM	24	Magnetic system release	The release mechanism shall be equipped with 4 Uxcell 12V 25N lifting magnets able to lift the cleaning rover to and from the solar panels	Secure payload
	25	Pivot system	The release mechanism shall include a motorized pivot system equipped with a Muzei 20KG Servo Motor High Torque that can precisely tilt the plate to release the rover at the right moment, without requiring manual intervention.	Release control
	26	Release system	The release mechanism should ensure a controlled and smooth release of the rover, preventing sudden movements or jerks that could damage the rover or solar panel.	Panel safety
DRONE	27	Flight performance	The drone shall be able to fly in stable conditions during low and moderate winds.	Stability during flight
	28	Operation	The drone shall be operated by remote control technology.	Ensure precise control
	29	Camera system	The drone shall be equipped with a camera allowing the operator to see where it is flying.	Visual feedback
	30	Thrust generation	The propellers must be capable of generating sufficient thrust (2700 g each) to lift the drone with its payload, ensuring stable flight performance across various operating conditions.	Provide lift

## Appendix C

### High Level System Requirements

*Table 21: High Level System Requirements.*

System Requirements (High Level)				
Category	Sub-Category	Description	Requirement	Description / Validation
Function	Sensor	Sensors in this system should capture and provide relevant, accurate, precise, real-time data under standard operation conditions	Input / Output processing	Sensor systems shall process input and output data to ensure accurate conversion from analog to digital and interpretation, as well as vice versa.
			Power supply	Sensors shall receive the correct levels of voltage and current to operate properly under all standard operating conditions.
			Error Handling	Sensors shall autonomously recognize and handle certain predefined errors to maintain continuous operation.
	Communications	Communication should be standardized, accurate, precise, real-time and timely	Establish Standard Communication protocols	The system shall establish standardized communication protocols to ensure consistent data exchange.
			User - Drone Communication	The system shall support real-time remote control communications and video streaming from the drone.
			User - Rover Communication	The system shall notify the user when the rover has completed cleaning and allow for emergency stop or restart commands from the operator.
			Redundant Communication	The system shall provide redundant communication pathways to ensure data exchange continues during primary channel failures.
	Control	Control should be Accurate, precise, Real-Time and Timely	Drone Flight control system	The control system shall support drone stabilization and movement with precision and accuracy.
			Drone RC Input / Output Processing	The control system shall manage drone movement and hovering accurately based on RC inputs.
			Rover Autonomous control system	The control system shall autonomously control the rover's path, obstacle avoidance, edge detection, and cleaning actions.
			Rover Input / Output processing	The rover's input/output processing shall manage edge detection, cleaning completion validation, and communication with the drone.
			Drone Safety Control	The control system shall include safety protocols that autonomously land the drone if communication is lost and/or enters a fault state.
Reliability	Motor	Motors should be efficient, precise & responsive	Input processing	Motors shall process inputs into appropriate PWM or DC signals to control movement accurately.
			Power Supply	Motors shall receive the correct voltage and current levels to operate efficiently and reliably.
			Voltage / Current Regulation	Sensors shall receive a consistent and regulated supply of voltage and current to ensure reliable operation over time.
	Sensor	Sensors in this system should be consistent & reliable over time	Input / Output Noise Processing	Sensors shall include noise filtering to minimize interference and maintain signal integrity.
			Diagnosis / Health	Sensor system shall perform diagnostics to detect malfunctions or degradation and report issues to the control system.
			Communication Noise filtering	Communication systems shall filter noise to ensure clear and reliable signal transmission.
	Communications	Communication should remain stable, consistent & reliable over time	Latency	Communication systems shall meet latency requirements to support fast, real-time, and reliable interactions.
			Communication Recovery	The communication system shall automatically re-establish connection after a disruption and resume data transmission without data loss.
			Drone Stabilization	The control system shall implement a robust self-stabilization algorithm for the drone.
Reliability	Control	Control should be stable, consistent & reliable over time	Rover Pathing Efficiency	The rover control system shall maximize cleaning efficiency while minimizing cleaning time through optimized pathing.
			Control Fault Tolerance	The control system shall have fault tolerance mechanisms to detect and handle faults autonomously, minimizing impact on performance.
			Battery Monitoring	The control system shall monitor battery levels and notify the operator if the battery level drops below a critical threshold.
			Voltage / Current Regulation	Motors shall receive regulated voltage and current to ensure stable and consistent operation over time.
	Motor	Motor should provide stable, consistent & reliable operation over time	Input / Output Noise Processing	Motor control systems shall implement noise filtering to reduce signal interference.
			Motor Feedback Monitoring	Motors shall have monitoring mechanisms for RPM and temperature to detect performance issues and prevent overheating.

## Appendix D

### Subsystem Requirements

*Table 22: Subsystem Requirements.*

System Requirements (Sub-System Level breakdown)				
Systems	Subsystems	Description	Requirement	Description / Validation
Remote Control	Rover Release - Capture Control	Control rover release and capture mechanisms	Rover Release Mechanism	The system shall include a mechanism to secure the rover in flight, which disengages upon landing.
			Release Mechanism Control	The system shall allow for user-initiated release or capture of the rover via remote control commands.
			RF Module Communication	The system shall use RF communication to send and receive real-time release and capture commands from the operator.
	User Flight Control	Real-time drone control by the user	User-Controlled Flight Operations	The system shall respond to real-time RC commands for take-off, hovering, landing, and movement control with high precision and low latency.
Release - Capture	Release - Capture	Mechanism for secure drone-rover capture	Video Streaming Module	The system shall provide real-time video streaming to the operator using a camera module, facilitating remote flight control.
			Electro-Magnet Lifting	An electromagnet shall be used to hold and release the rover, deactivating to release and activating to pickup again on command.
			Drone Position and Movement Accuracy	The system shall support real-time movement controls with precise adjustments to stabilize and maintain course based on user input.
	User Flight Control	Real-time drone control by user	Self-Stabilization Algorithm	The control system shall implement an autonomous stabilization algorithm that adjusts the drone's pitch, roll, and yaw to maintain stable flight while responding to user input.
Flight	Autonomous Flight Stabilization	Autonomous drone stability control	IMU Integration	The flight system shall use an IMU for accurate stabilization by providing real-time orientation (roll,pitch, yaw) and acceleration data.
			Weight Management Algorithm	An algorithm shall be implemented to manage payload balance, adjusting flight parameters to account for the rover's weight.
			Obstacle Avoidance and Edge Detection	The system shall detect obstacles and edges, autonomously adjusting path to avoid falls and collisions while covering target surfaces.
	Rover Movement	Rover's movement and navigation on surfaces	Position Tracking System	The rover shall utilize sensors to track its position on the cleaning grid and maintain accuracy throughout operation.
Autonomous Pathing	Rover Positioning	Accurate tracking of rover position	Optimized Path Mapping	The rover control system shall utilize an optimized route mapping algorithm to maximize coverage while minimizing redundant passes and time.
	Rover Route Mapping	Efficient and complete cleaning route generation	Cleaning Validation	The system shall verify cleaning task completion and communicate the status back to the user upon task end.
	Cleaning	Execution of solar panel cleaning tasks	Cleaning Contact Control	Cleaning mechanisms shall ensure proper & accurate contact with the solar panel to guarantee optimal cleaning.
Communication	Drone - Operator	Communication between drone and user	Brush Motor Control	The cleaning module shall control brush motor speed and pressure to optimize cleaning without damaging the panels.
			Drone-User Communication	The system shall support real-time communication with the user for status updates, video feeds, and control commands.
	Rover - Operator	Communication between rover and user	RF Module for Remote Control	An RF module shall be used to ensure reliable real-time data transmission between the drone and operator.
			Rover Status Notifications	The system shall notify the user of the rover's progress, cleaning completion, and system status, allowing for emergency stops or task adjustments.
Circuiting	Power Control	Power distribution and regulation	Communication Protocol	The system shall implement/use a standardized communication protocol to manage data exchange between the drone, rover, and operator.
			Voltage and Current Regulation	The PCB shall include regulated voltage and current lines, ensuring that sensors, motors, and control systems receive stable power under all operating conditions.
			PCB Structural Integrity	The PCB shall include mounting points, limit switch input buses, test points, and support for modular add-ons.
			Signal Isolation and Filtering	The system shall use internal filters to prevent interference between communication, control, and sensor signals.
	Internal Signal Processing & transmission	Reliable signal processing and data exchange	PWM Control and Analog Input Support	The PCB shall support PWM and analog inputs to control motor speed and sensor readings.
			Noise Filtering and Error Handling	The system shall include noise filters to minimize interference, and error handling mechanisms to detect and address data errors in signal processing.
	Internal Data Exchange	Data exchange within system components	Inter-Module Communication Protocol	The PCB shall support a communication protocol for consistent data transmission between control, power, and sensor systems.
			Interrupt Handling	The control bus shall handle interrupt signals for prioritizing critical actions, such as emergency landings or system fault alerts.
			Diagnostics Algorithm/Circuit	The PCB shall include diagnostics to monitor system health and performance, alerting the operator of any malfunctions.

## Appendix E

### Detailed Drawing of the Drone

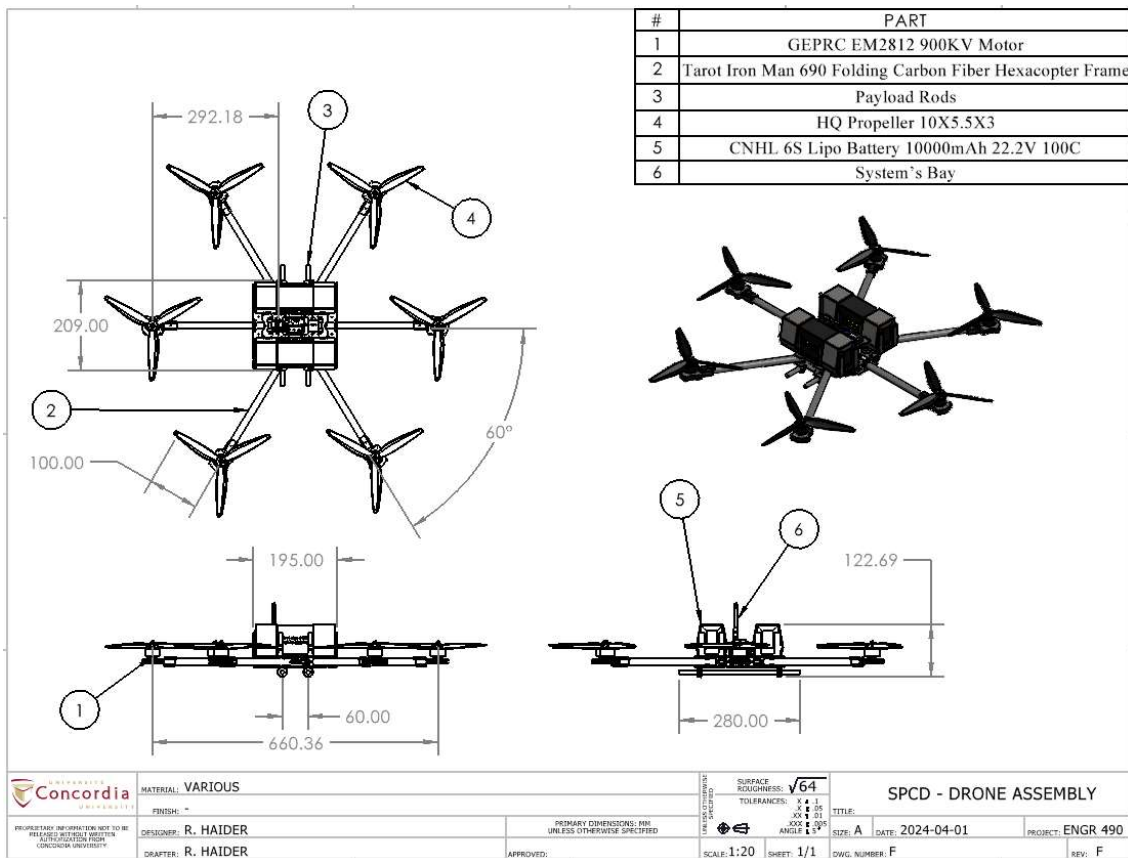


Figure 58. Detailed Drawing of the Drone.

## Appendix F

### Landing Gear Drawings

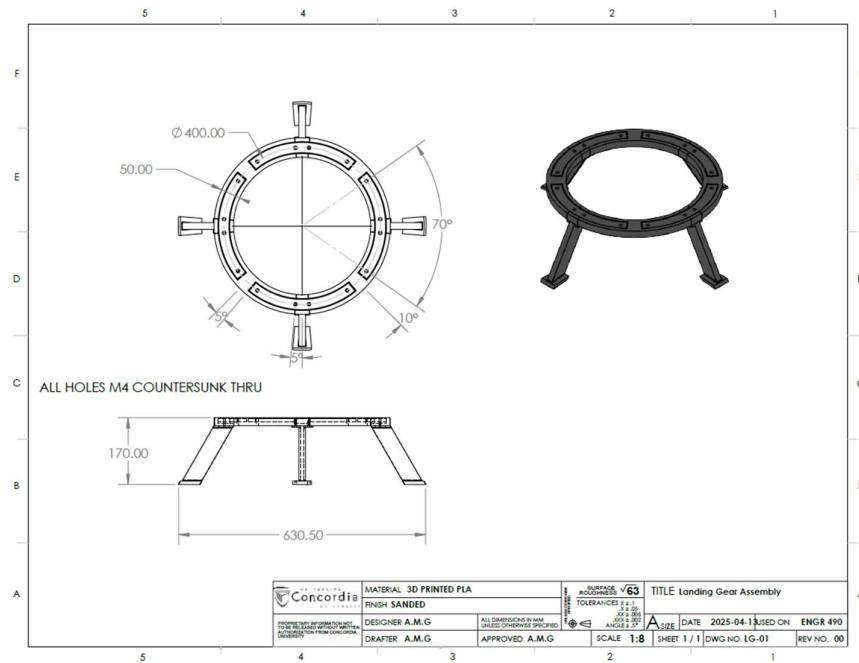


Figure 59: Landing Gear Assembly Drawing

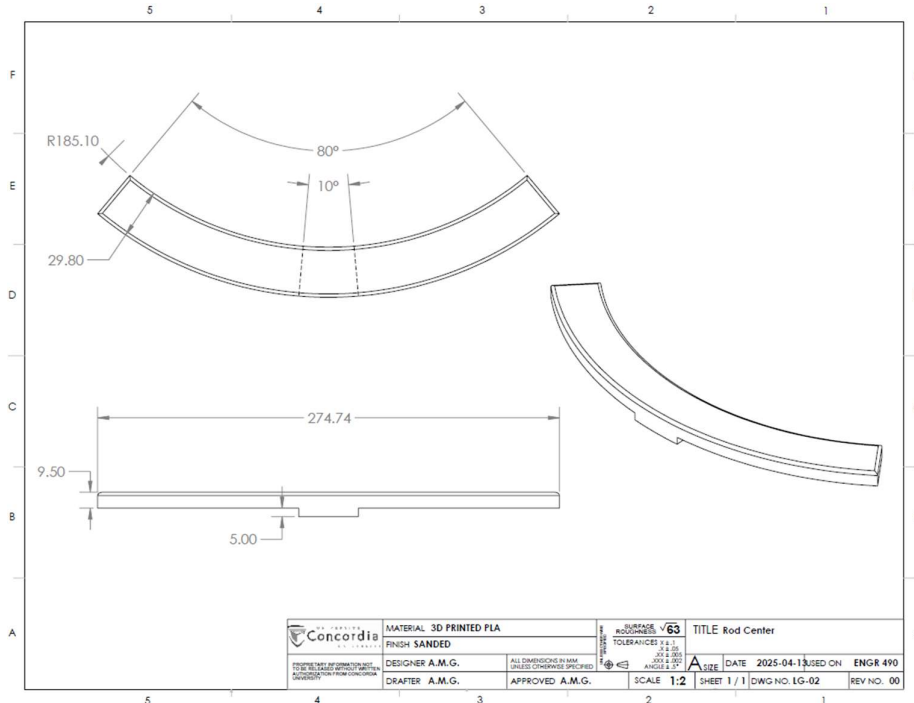


Figure 60: Landing Gear Drawing - Rod Center

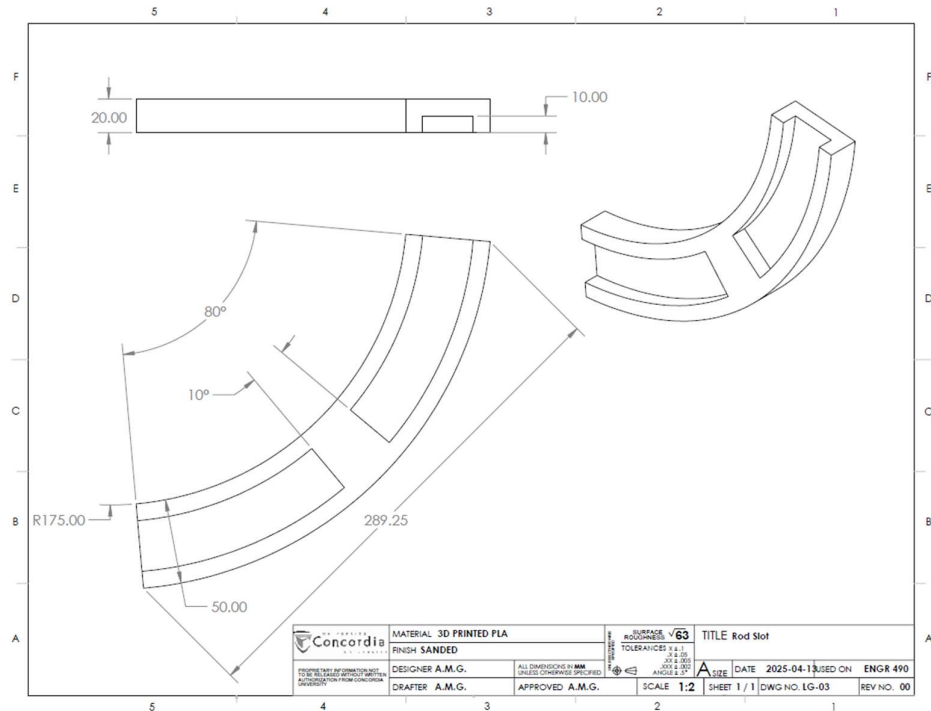


Figure 61: Landing Gear Drawing - Rod Slot

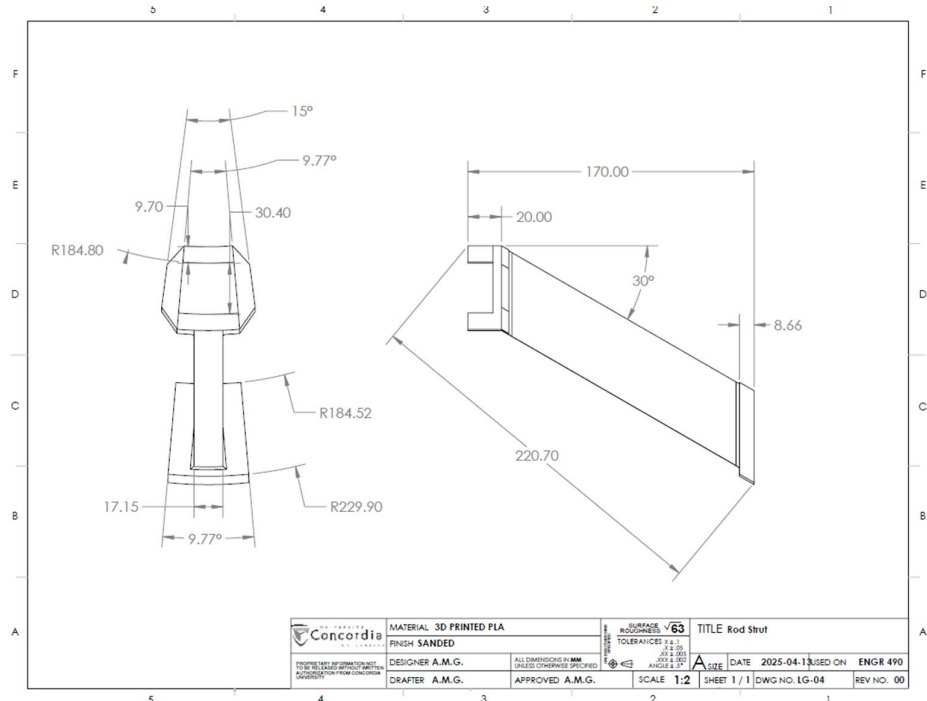


Figure 62: Landing Gear Drawing - Rod Strut

## Appendix G

### Detailed Drawing of the Rover Fuselage

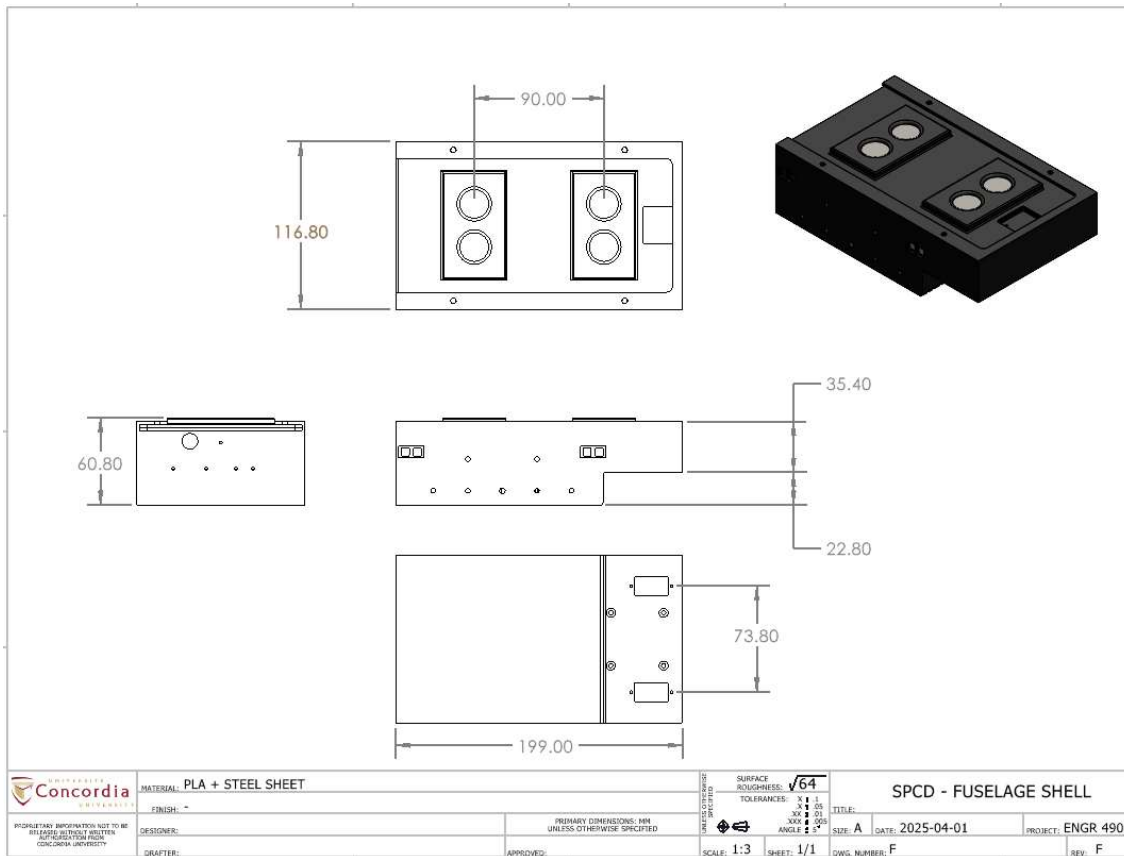


Figure 63: Detailed drawing of the rover fuselage

## Appendix H

### Detailed Drawing of the Rover Displacement System

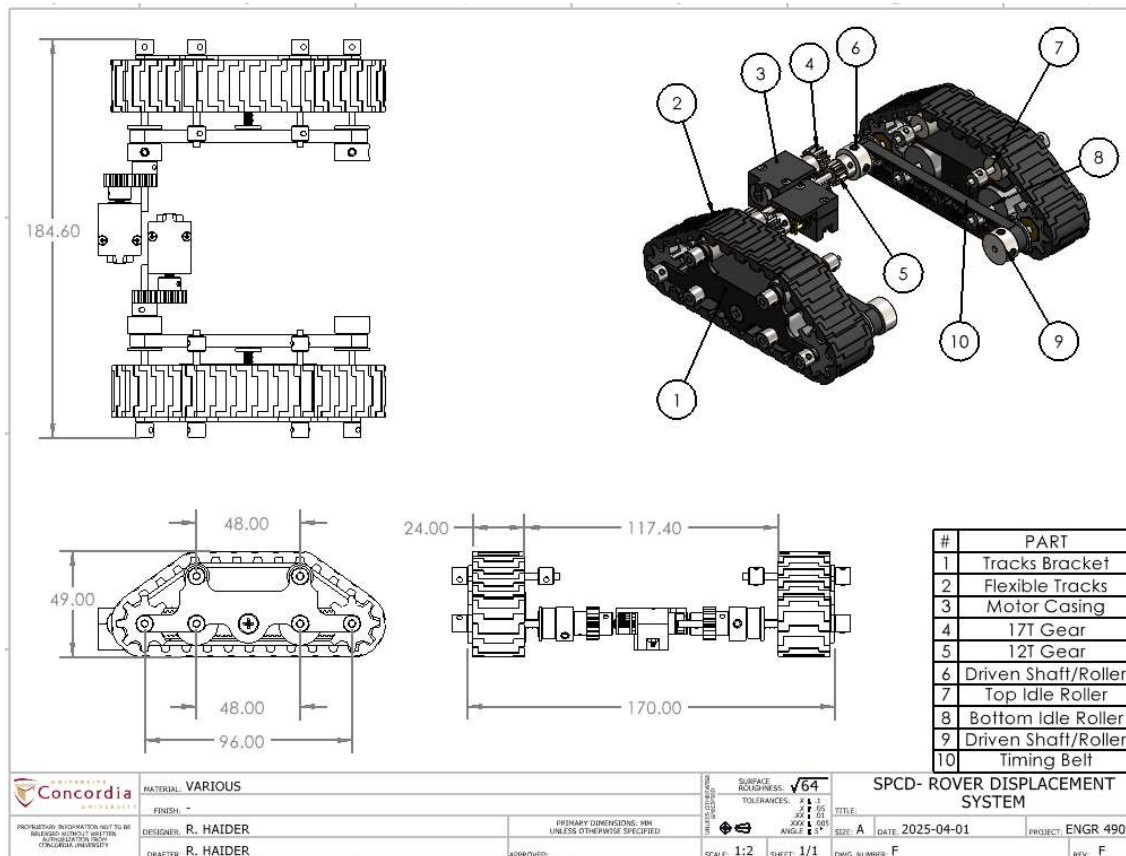


Figure 64: Detailed Drawing of the Rover Displacement System.

## Appendix I

### Brush System Drawing

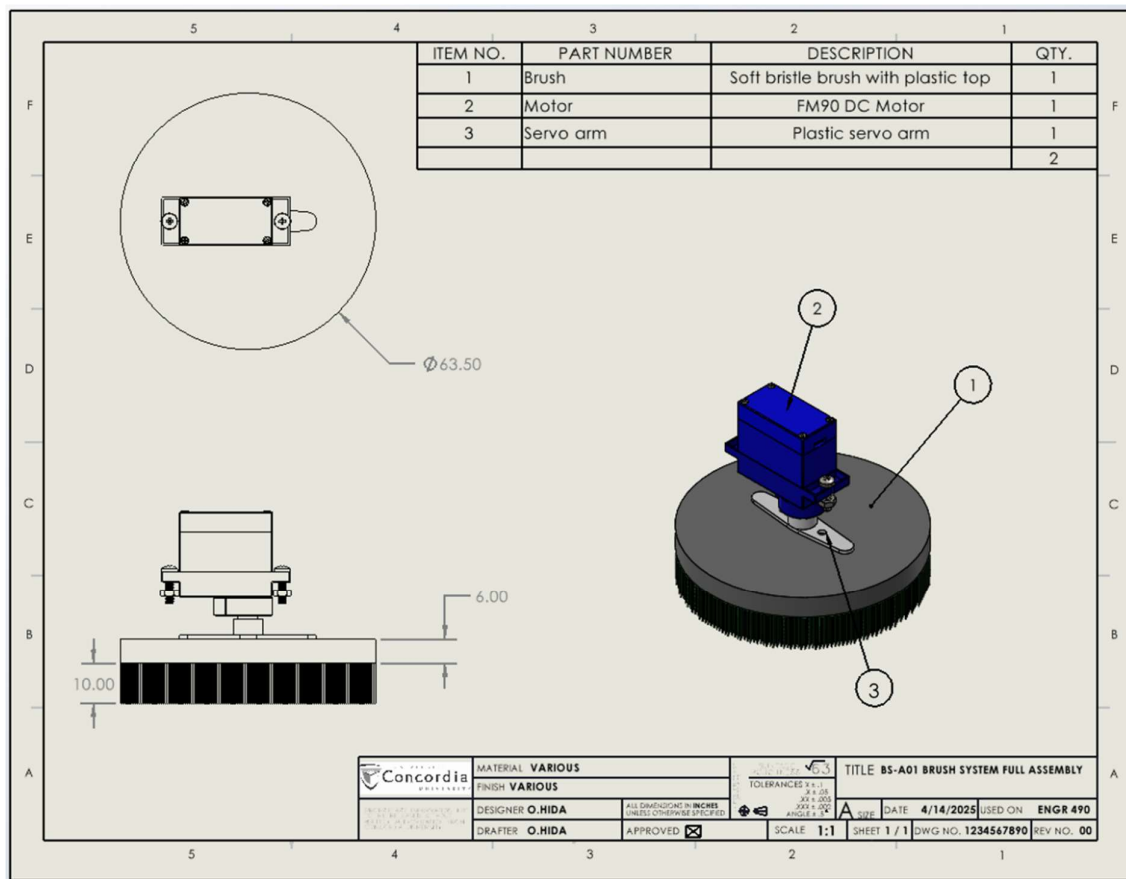


Figure 65: Brush System Drawing.

## Appendix J

### Back Cloth Drawing

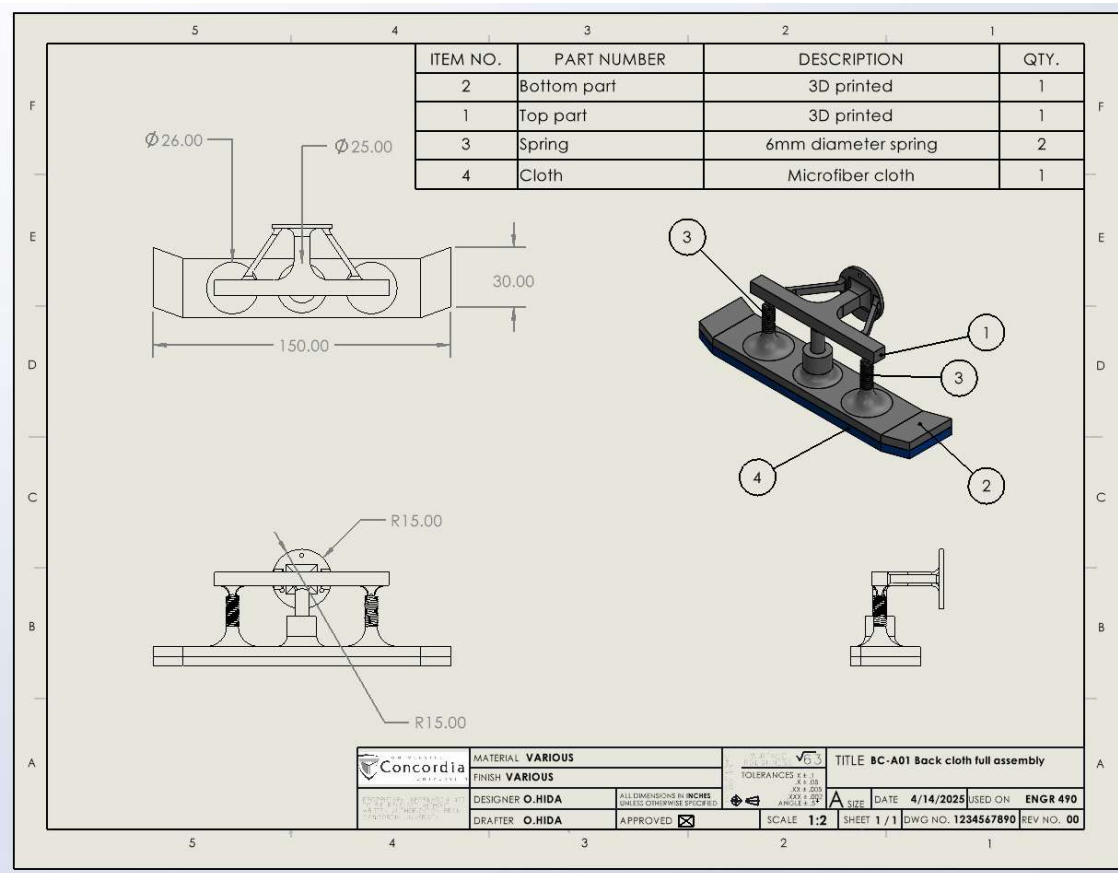


Figure 66: Back Cloth Drawing.

## Appendix K

### Rover System Schematics

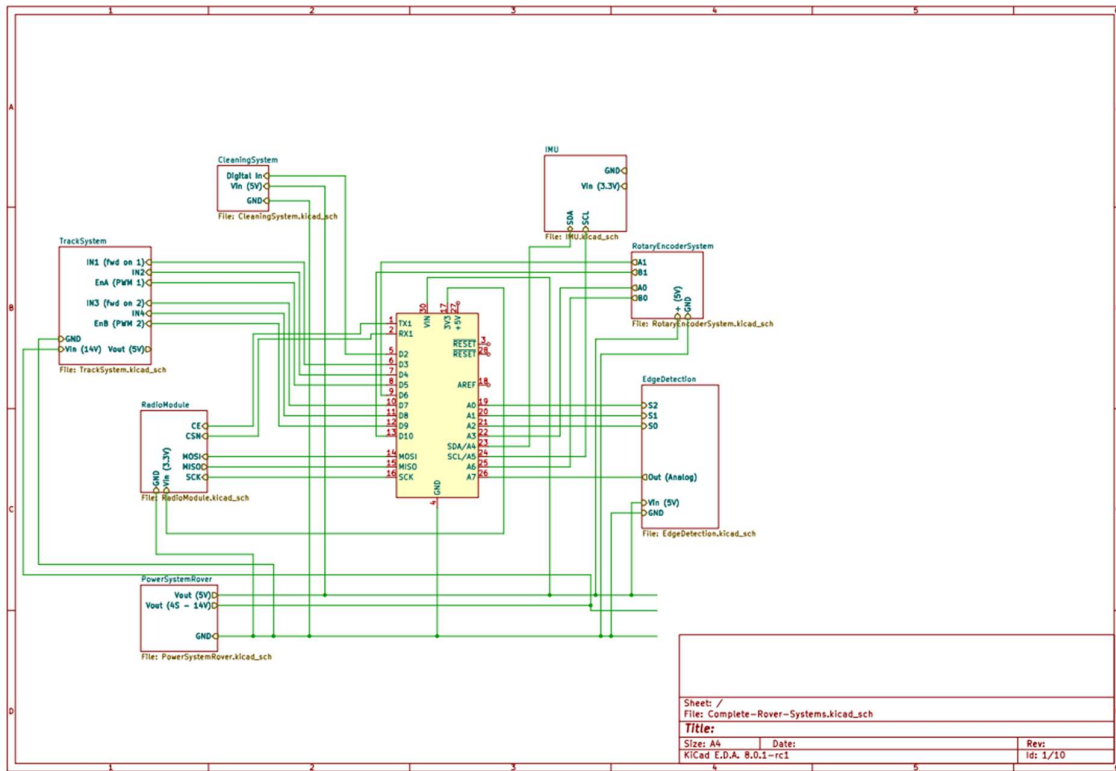


Figure 67: Complete Rover Systems KiCad.

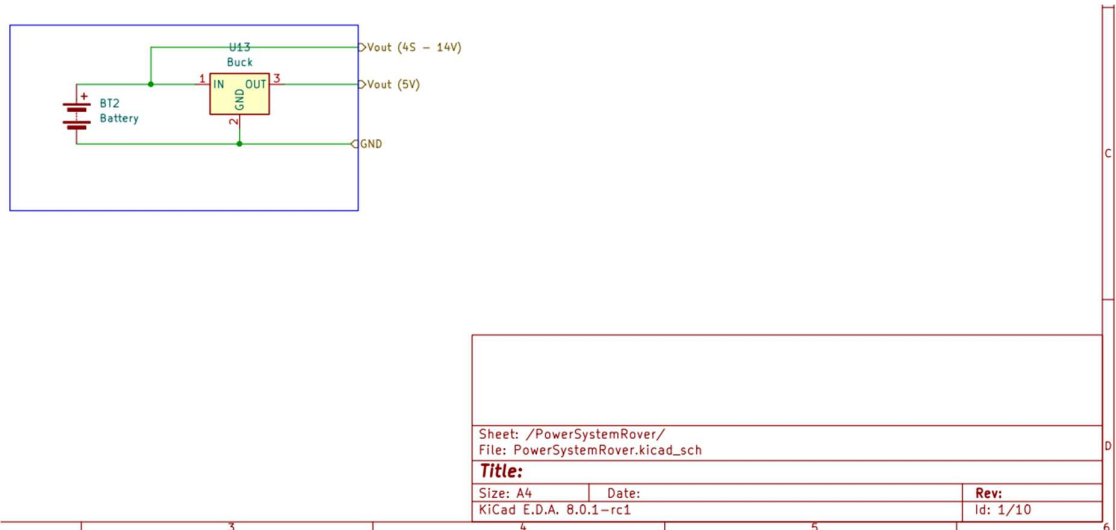


Figure 68: Power System Rover KiCad.

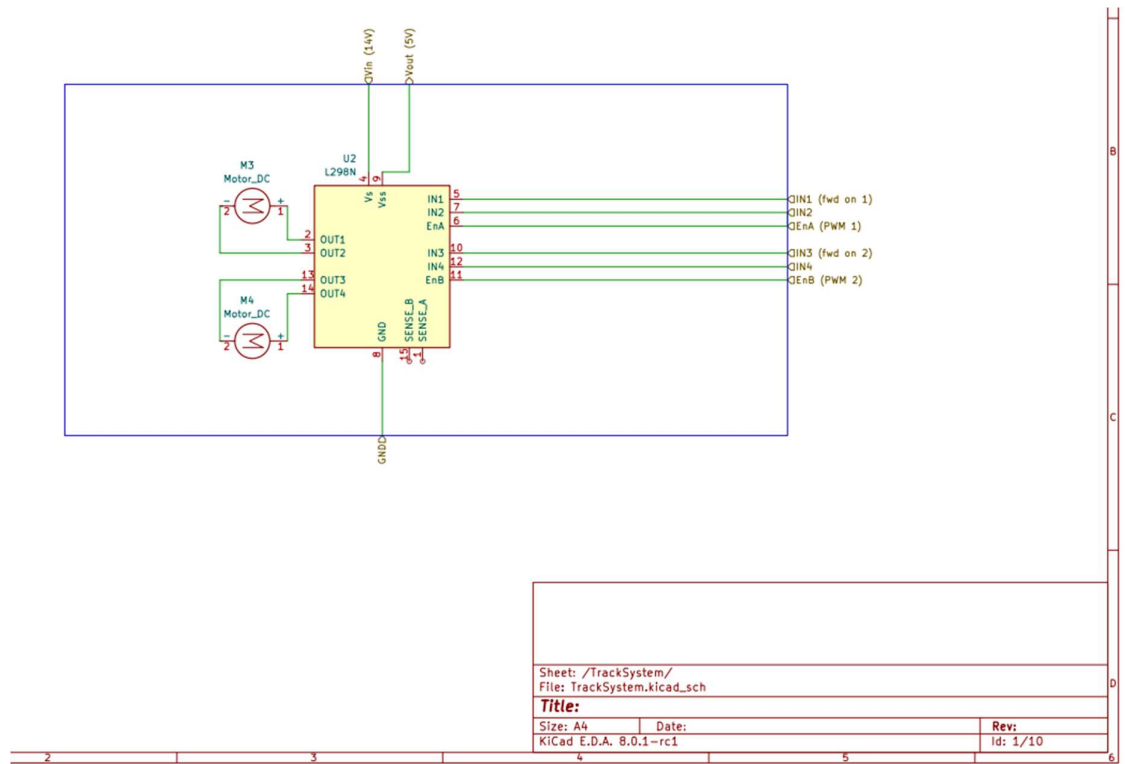


Figure 69: Track System KiCad.

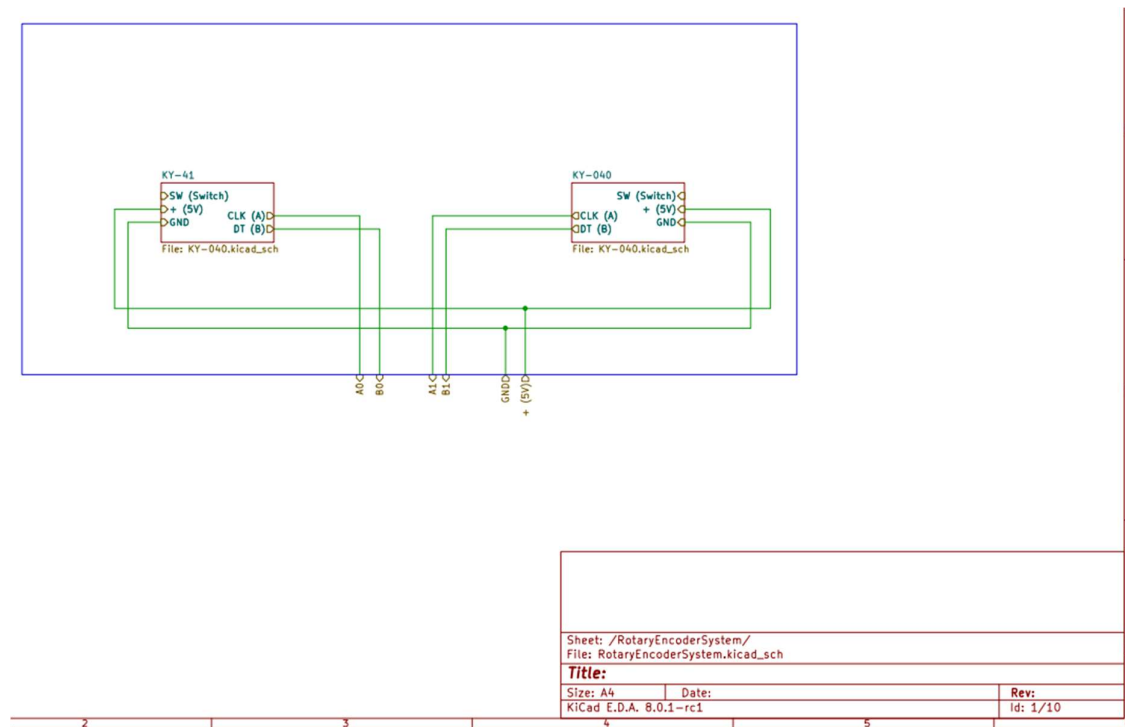


Figure 70: Rotary Encoder System KiCad.

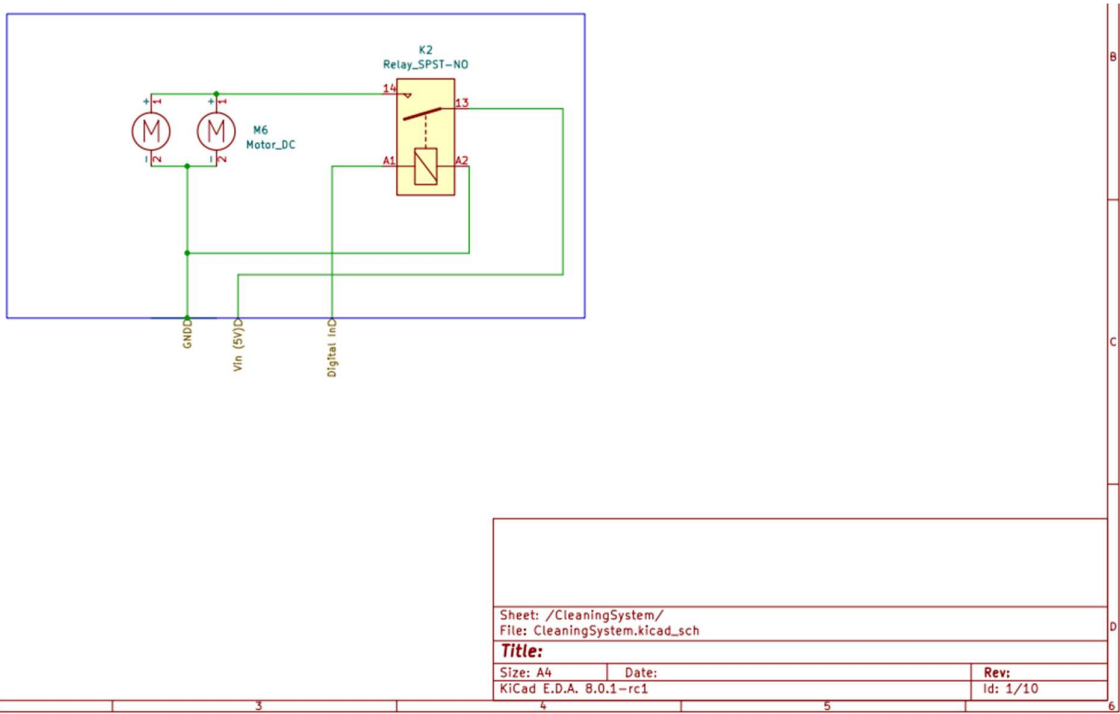


Figure 71: Cleaning System KiCad.

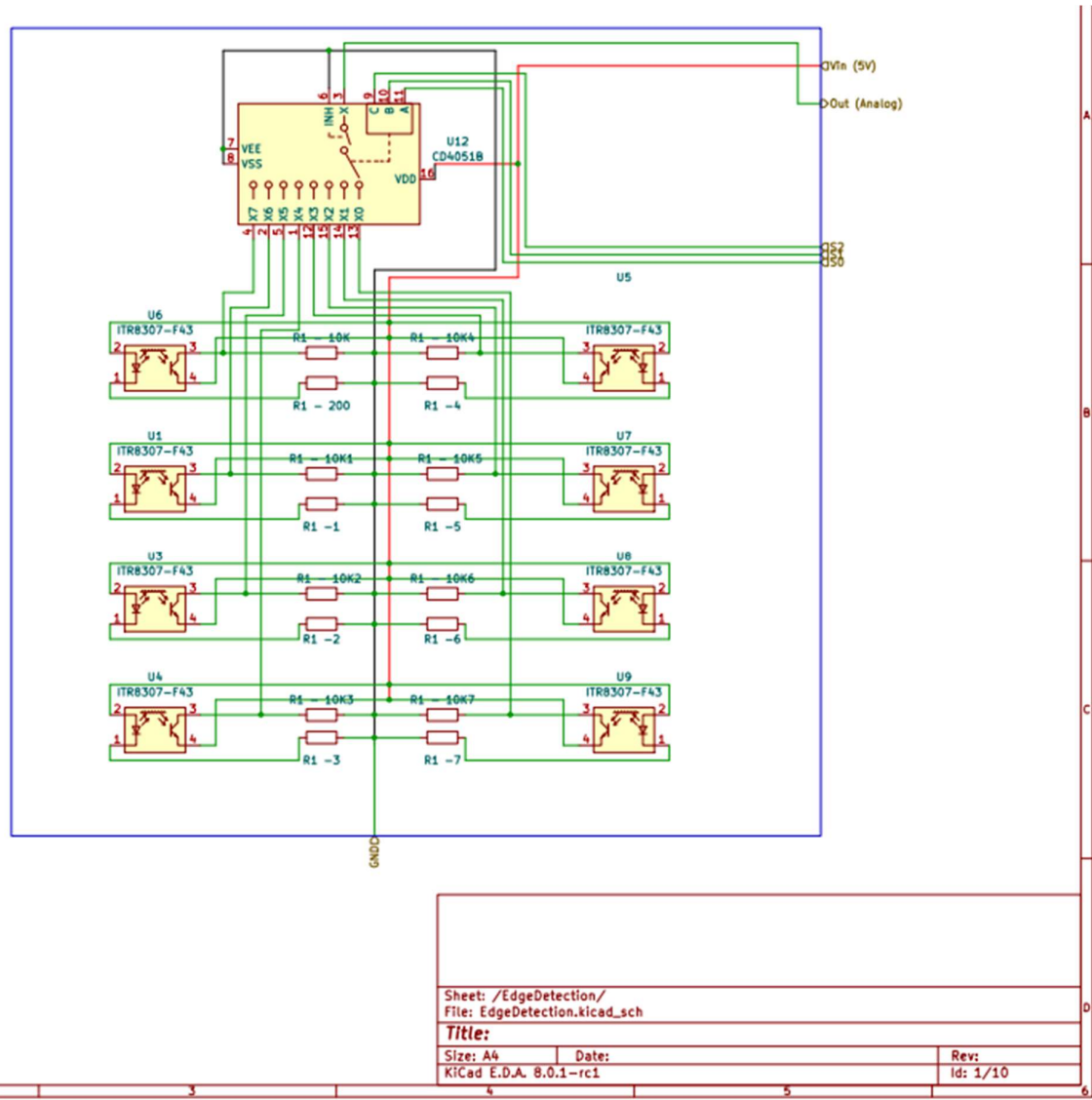


Figure 72: Edge Detection KiCad.

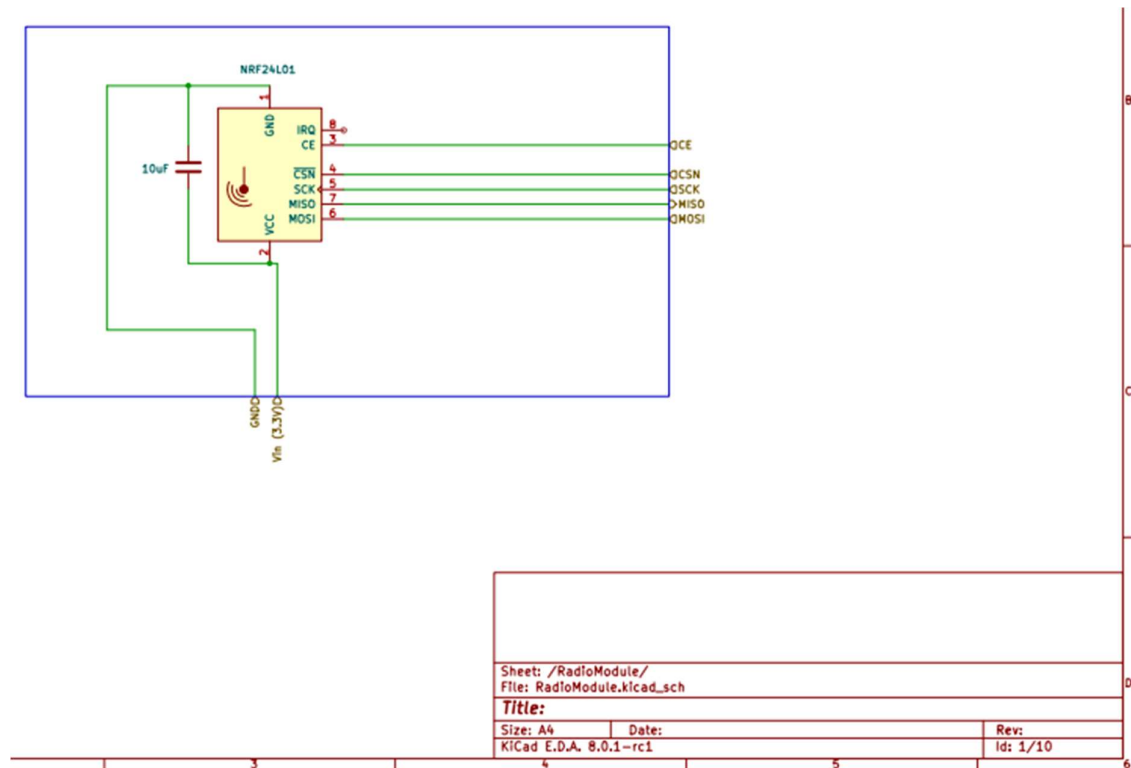
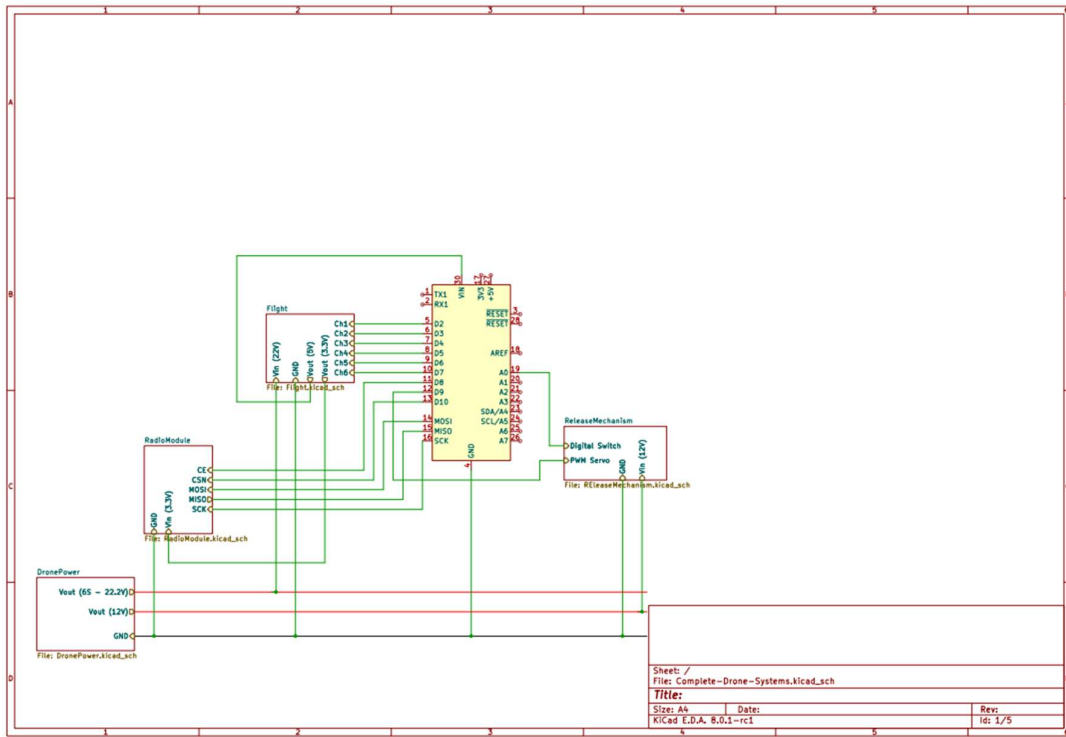


Figure 73: Radio Module KiCad.

## Appendix L

### Drone System Schematics



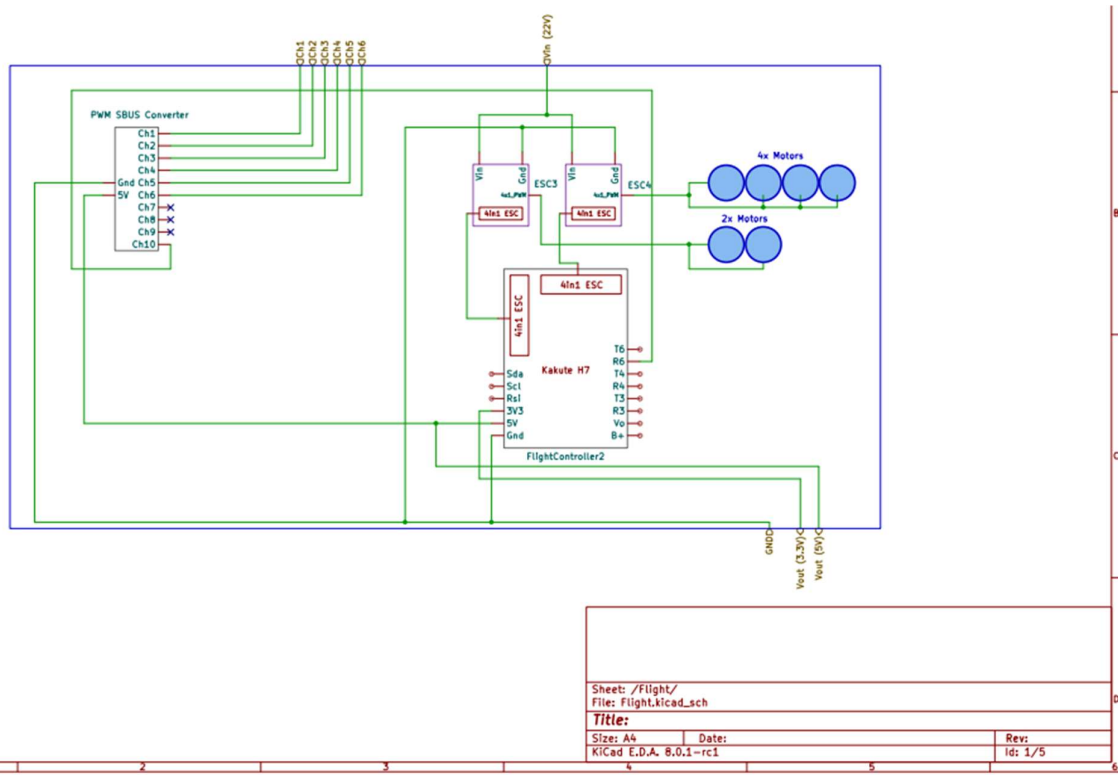


Figure 76: Flight KiCad.

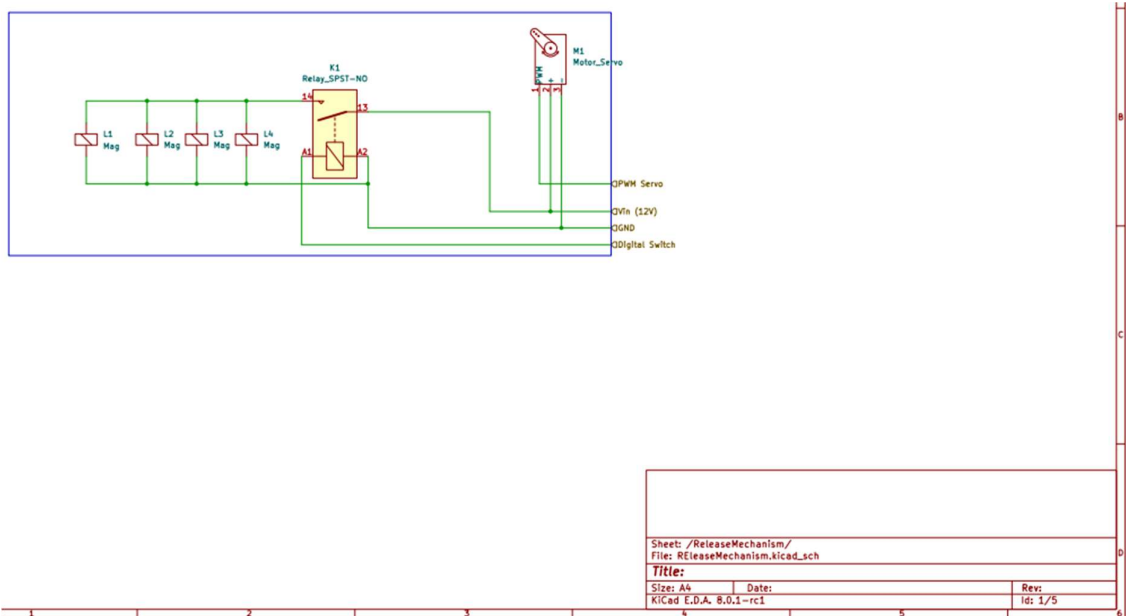


Figure 77: Release Mechanism KiCad.

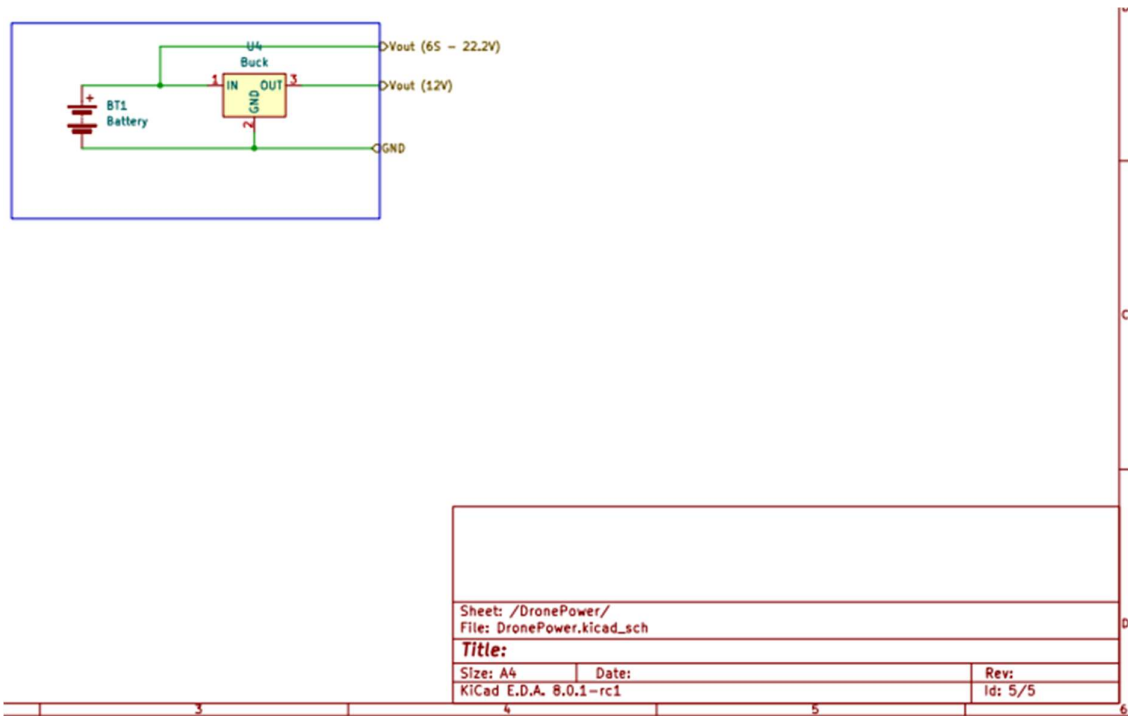


Figure 78: Drone Power KiCad.